Seismic Inversion: Reading Between the Lines

Frazer Barclay
Perth, Western Australia, Australia

Anders Bruun
Klaus Bolding Rasmussen
Copenhagen, Denmark

Jose Camara Alfaro
Pemex
Tampico, Tamaulipas, Mexico

Anthony Cooke
Aberdeen, Scotland

Dennis Cooke
Darren Salter
Santos
Perth, Western Australia

Robert Godfrey
Dominic Lowden
Steve McHugo
Hüseyin Özdemir
Stephen Pickering
Gatwick, England

Francisco Gonzalez Pineda
Pemex
Reynosa, Tamaulipas, Mexico

Jorg Herwanger
Stefano Volterrani
Houston, Texas, USA

Andrea Murineddu
Andreas Rasmussen
Stavanger, Norway

Ron Roberts
Apache Corporation
Calgary, Alberta, Canada

The reflections of seismic waves from subsurface layers illuminate potential hydrocarbon accumulations. As waves reflect, their amplitudes change to reveal important information about the underlying materials. Seismic amplitude inversion uses reflection amplitudes, calibrated with well data, to extract details that can be correlated with porosity, lithology, fluid saturation and geomechanical parameters.

The undisputed leader among tools for identifying potential exploration targets is the 3D seismic survey. These surveys probe great volumes of the subsurface, helping oil and gas companies map geological structures and select drilling locations.

The original use of seismic data, and still the main use today, has been to identify the geometry of reflectors and ascertain their depths. This is possible because seismic waves reflect at interfaces between materials of different acoustic properties.

However, seismic reflection data contain information beyond reflector location: every reflection changes the amplitude of the returned wave. The controlling property in this change at the interface is the contrast in impedance, which is the product of density and velocity. Seismic reflection amplitude information can be used to back out, or invert for, the relative impedances of the materials on both sides of the interface. By correlating these seismically derived properties with values measured in the borehole, interpreters may be able to extend well information throughout the entire seismic volume. This process, called seismic inversion for reservoir characterization, can help fill gaps in our knowledge of formation properties between wells.

This article describes the science and art of seismic inversion, and how oil and gas companies are using it to reduce risk in their exploration, development and production operations. After an introduction to the uses of inversion, we present its various types, from simple to more complex. Examples from Mexico, Egypt, Australia and the North Sea demonstrate applications of inversion to fine-tune drilling locations, characterize hard-to-image reservoirs, map water saturation, improve reservoir simulations and enhance knowledge of geomechanical properties.

Inversion Basics

Many measurements in the E&P industry rely to some extent on inversion for their interpretation. The reason is simple. For several measurement-interpretation problems, no equation that directly relates the multiple measurements—which include noise, losses and other inaccuracies—can be solved with a unique answer. We then resort to inversion, which is a mathematical way of estimating an answer, checking it against observations and modifying it until the answer is acceptable.

For help in preparation of this article, thanks to Trine Alsos, StatoilHydro, Harstad, Norway; Ted Bakamjian, SEG, Tulsa; Richard Bottomley, Mexico City; Jonathan Bown, Henrik Juhl Hansen and Kim Gunn Maver, Copenhagen; Tim Bunting, Kuala Lumpur; Karen Sullivan Glaser, Houston; Jalal Khazanehdari, Abu Dhabi, UAE; Hasbi Lubis, Gatwick, England; Farid Mohamed, Aberdeen; Richard Patenall, Perth, Western Australia; Pramesh Tyagi, Cairo; and Anke Simone Wendt, Stavanger.

1. Quirein J, Kimminau S, La Vigne J, Singer J and Wendel F: "A Coherent Framework for Developing and Applying Multiple Formation Evaluation Models," *Transactions of the SPWLA 27th Annual Logging Symposium*, Houston, June 9–13, 1986, paper DD.

Jammes L, Faivre O, Legendre E, Rothnemer P, Trouiller J-C, Galli M-T, Gonfalini M and Gossenberg P: "Improved Saturation Determination in Thin-Bed Environments Using 2D Parametric Inversion," paper SPE 62907, presented at the SPE Annual Technical Conference and Exhibition, Dallas, October 1–4, 2000.

Faivre O, Barber T, Jammes L and Vuhoang D: "Using Array Induction and Array Laterolog Data to Characterize Resistivity Anisotropy in Vertical Wells," *Transactions of the SPWLA 43rd Annual Logging Symposium*, Oiso, Japan, June 4–7, 2002, paper M.

Marsala AF, Al-Ruwaili S, Ma SM, Modiu SL, Ali Z, Donadille J-M and Wilt M: "Crosswell Electromagnetic Tomography in Haradh Field: Modeling to Measurements," paper SPE 110528, presented at the SPE Annual Technical Conference and Exhibition, Anaheim, California, USA, November 11–14, 2007.

Inversion, as the name implies, can be considered as the inverse of forward modeling, sometimes simply called modeling. For the purpose of this article, forward modeling begins with a model of earth properties, then mathematically simulates a physical experiment or process—for example, electromagnetic, acoustic, nuclear, chemical or optical—on the earth model, and finally outputs a modeled response. If the model and the assumptions are accurate, the modeled response looks like real data. Inversion does the reverse: it starts with actual measured data, applies an operation that steps backward through the physical experiment, and delivers an earth model. If the inversion is done properly, the earth model looks like the real earth.

Inversion is used by many E&P disciplines and can be applied at a wide range of scales and varying levels of complexity:

- calculating borehole-fluid invasion profiles from induction logging measurements
- assessing cement-bond quality from ultrasonic logs (see "Ensuring Zonal Isolation Beyond the Life of the Well," *page 18*).
- extracting layer lithologies and fluid saturations from multiple log measurements
- interpreting gas, oil and water volumes from production logs
- inferring reservoir permeability and extent from pressure-transient data (see "Intelligent Well Technology in Underground Gas Storage," *page 4*).
- mapping fluid fronts from crosswell electromagnetic measurements
- integrating electromagnetic and seismic measurements for improved delineation of subsalt sediments.[1]

E&P seismic specialists use different types of inversion—velocity inversion and amplitude inversion—to solve distinct types of problems. The first type of inversion, velocity inversion, sometimes known as traveltime inversion, is used for depth imaging. Using seismic traces at widely spaced locations, it generates a velocity-depth earth model that fits recorded arrival times of seismic waves. The result is a relatively coarse velocity-depth model extending over several kilometers in depth and perhaps hundreds of kilometers in length and width. This solution is applied in data-processing steps such as migration and stacking, eventually producing the type of seismic image that is familiar to most readers. Seismic interpreters use these images to determine the shape and depth of subsurface reflectors.

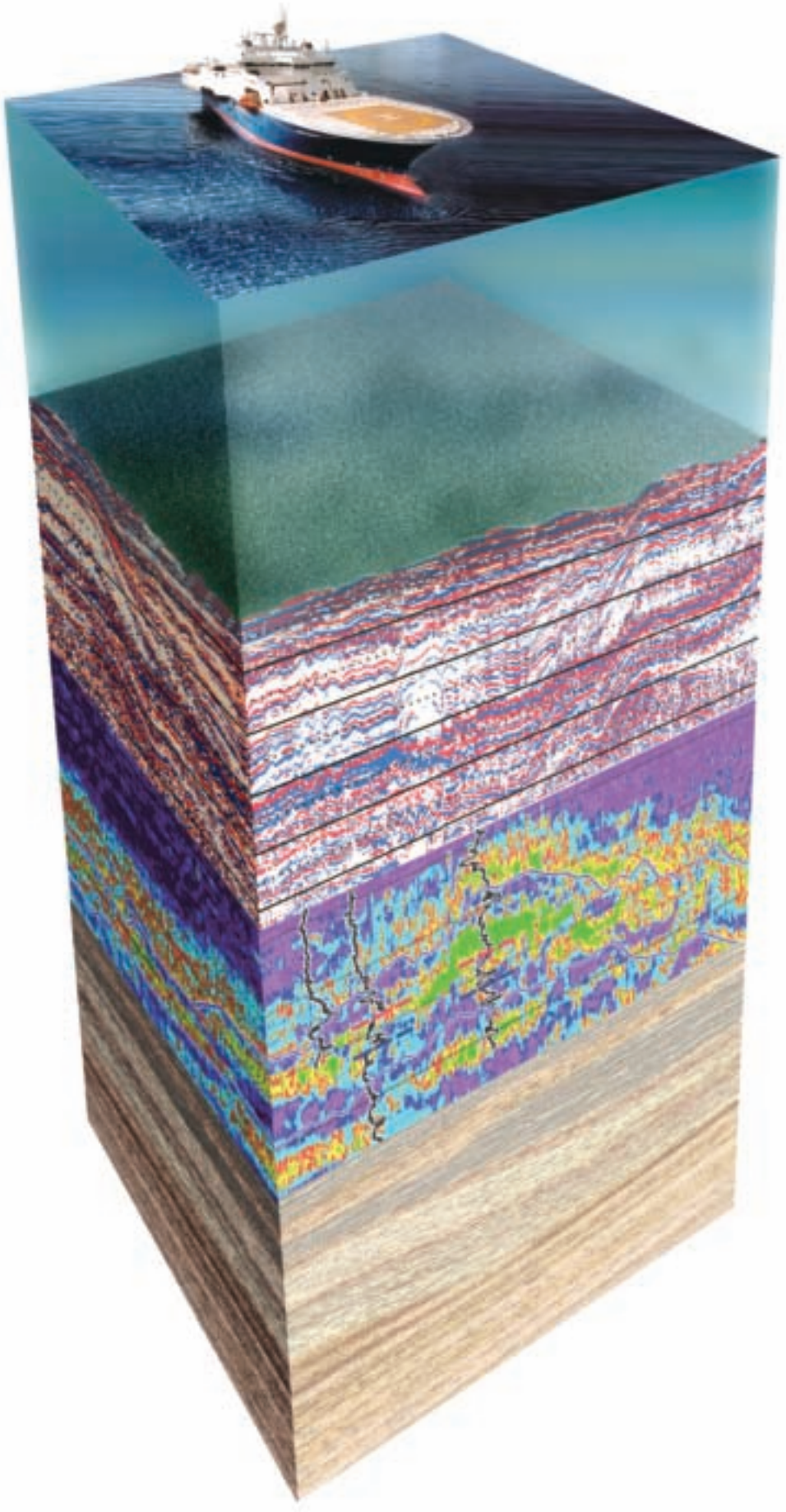

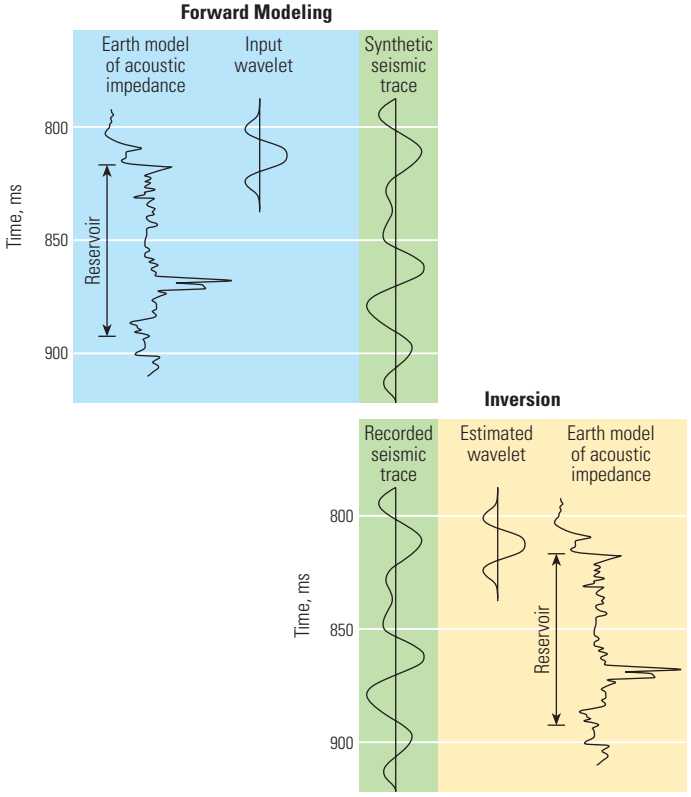

^ Modeling and inversion. Forward modeling (*top*) takes a model of formation properties—in this case acoustic impedance developed from well logs—combines this with a seismic wavelet, or pulse, and outputs a synthetic seismic trace. Conversely, inversion (*bottom*) begins with a recorded seismic data trace and removes the effect of an estimated wavelet, creating values of acoustic impedance at every time sample.

The second type of inversion, amplitude inversion, is the focus of this article. This approach uses the arrival time and the amplitude of reflected seismic waves at every reflection point to solve for the relative impedances of formations bounded by the imaged reflectors. This inversion, called seismic inversion for reservoir characterization, reads between the lines, or between reflecting interfaces, to produce detailed models of rock properties. For simplicity, the following discussion describes only model-based inversion. Some other alternatives are space-adaptive and discrete spike inversions.[2]

In principle, the first step in model-based seismic inversion—forward modeling—begins with a model of layers with estimated formation depths, thicknesses, densities and velocities derived from well logs. The simplest model, which involves only compressional (*P*-wave) velocities (V_p) and density (ρ), can be used to invert for *P*-wave, or acoustic, impedance. Models that include shear (*S*-wave) velocities (V_s) can solve for *S*-wave, or elastic, impedance.

The simple model is combined with a seismic pulse to create a modeled seismic trace called a synthetic (above). Inversion takes an actual seismic trace, removes the seismic pulse, and delivers an earth model for that trace location. To arrive at the best-fit model, most inversion routines iterate between forward modeling and inversion, seeking to minimize the difference between the synthetic trace and the data.

In practice, each of these steps may be quite involved and can depend on the type of seismic data being inverted. For vertical-incidence data, creating the initial model requires bulk density measurements from density logs and compressional velocities from sonic logs, both spanning the interval to be inverted. Unfortunately, the necessary logs often are acquired only in the reservoir. In the absence of sonic logs, borehole seismic surveys—vertical seismic profiles (VSPs)—can provide average velocities across the required interval. If no borehole velocity data are available, velocities from traveltime inversion may serve as a substitute. Missing density data may be estimated from empirical relationships. For nonvertical-incidence data, the model must include both *S*-wave and *P*-wave velocities.

For conventional inversion of vertical-incidence data, the density-velocity model is then converted to a reflectivity model. Reflectivity, the ratio of the amplitude of the reflected wave to that of the incident wave, is the parameter that governs reflection-driven changes in normal-incidence seismic amplitudes. It relates to the densities and velocities on each side of an interface through the acoustic impedance contrast; reflectivity is the ratio of the difference in acoustic impedances to their sum.[3] The resulting depth-based reflectivity model is converted to a time-based model through the velocities.

Combining the time-based model with a seismic pulse creates a synthetic trace. Mathematically, this process is known as convolution.[4] The seismic pulse, or wavelet, represents the packet of energy arriving from a seismic source. A model wavelet is selected to match the amplitude, phase and frequency characteristics of the processed seismic data. Convolution of the wavelet with the reflectivity model yields a synthetic seismic trace that represents the response of the earth as modeled to the input seismic pulse. Additional steps are required if noise, attenuation and multiple reflections are to be included in the modeled trace.

The inverse operation starts with an actual seismic trace. Because the amplitude and shape of each swing in the seismic trace affect the outcome, it is vital that the processing steps up to this point conserve signal phase and amplitude.

Different types of inversion start with different types of traces. The main distinction is between inversion performed before stacking and inversion performed after it—prestack and poststack. Most seismic surveys provide images using data that have been stacked. Stacking is a signal-enhancement technique that averages many seismic traces. The traces represent recordings from a collection of different source-receiver offsets with a common reflecting midpoint (next page, top left). Each trace is assumed to contain the same signal but different random noise. Stacking produces a single trace with minimal random noise and with signal amplitude equal to the average of the signal in the stacked traces. The resulting stacked trace is taken to be the response of a normal-incidence reflection at the common midpoint (CMP).

2. "Space-Adaptive Inversion," http://www.slb.com/content/services/seismic/reservoir/inversion/space_adaptive.asp (accessed April 22, 2008).
3. Reflectivity may be positive or negative. Positive reflectivity means the reflected wave has the same polarity as the incident wave. Negative reflectivity means the reflected wave has the opposite polarity relative to the incident wave.
4. Yilmaz O and Doherty SM: *Seismic Data Processing*. Tulsa: Society of Exploration Geophysicists, 1987.

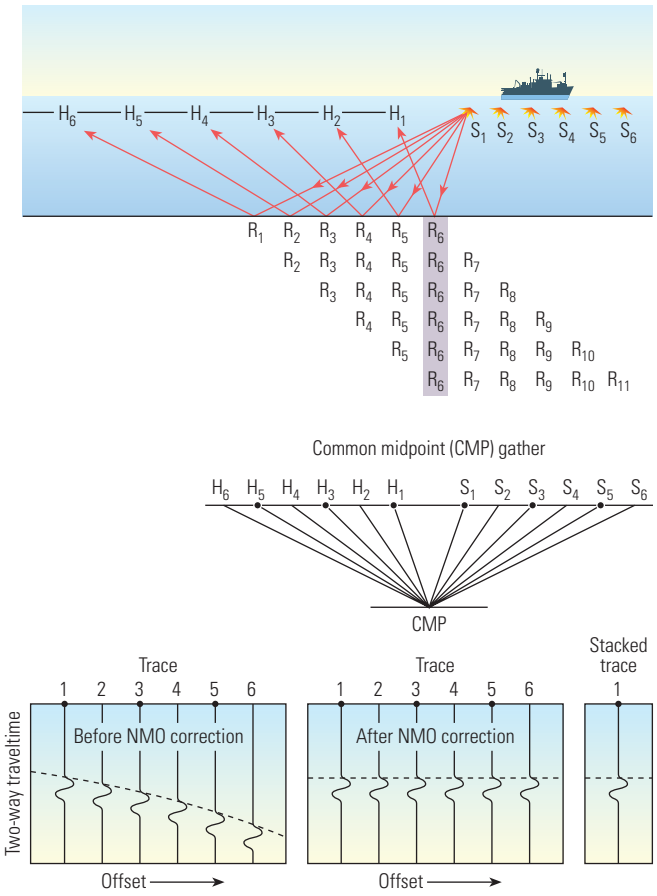

^ Stacking basics. Stacking enhances signal and reduces noise by adding several traces together. The seismic vessel acquires traces at many offsets from every source (*top*). S numbers represent sources, R numbers represent reflection points, and H numbers represent hydrophones. Stacking first gathers traces from all available source-receiver offsets that reflect at a common midpoint (CMP) (*middle*). Because arrivals from longer offsets have traveled farther, a time correction, called normal moveout (NMO) correction, is applied to each gather to flatten the arrivals (*bottom left*). The flattened traces are averaged (*bottom right*) to produce one stacked trace that represents the normal-incidence (zero-offset) trace.

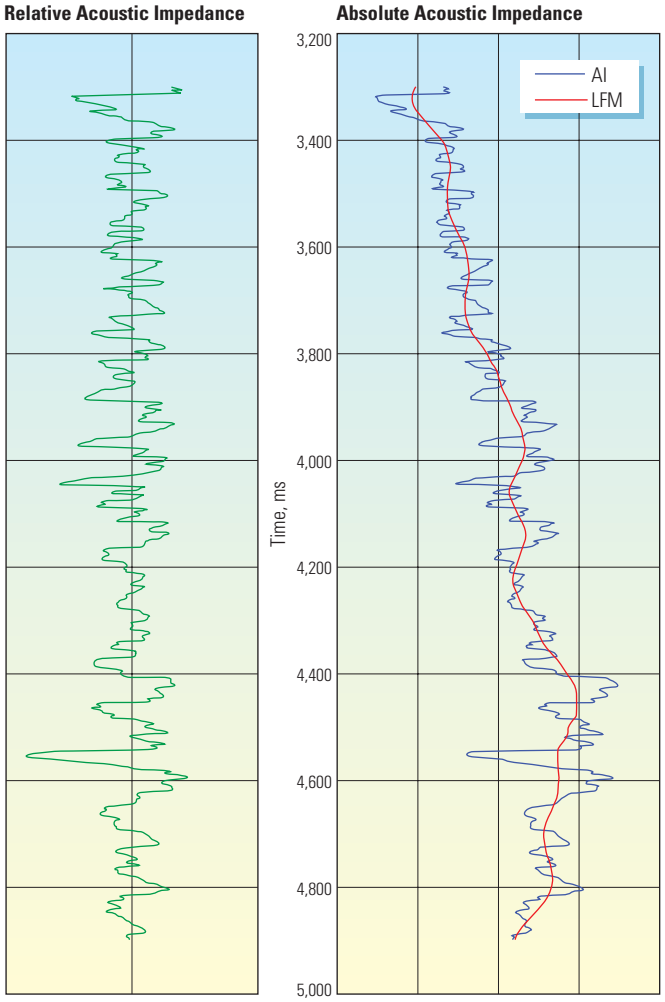

^ Relative and absolute acoustic impedance. Inversion of seismic amplitudes yields relative acoustic impedance (AI) (*left*). However, the true absolute acoustic impedance (blue) contains a low-frequency model (LFM) (red) that must be obtained from borehole data or modeled by other means (*right*).

Stacking is a reasonable processing step if certain assumptions hold: the velocity of the medium overlying the reflector may vary only gradually, and the average of the amplitudes in the stacked traces must be equivalent to the amplitude that would be recorded in a normal-incidence trace. In many cases, these assumptions are valid, and inversion may be performed on the stacked data—in other words, poststack. In contrast, when amplitude varies strongly with offset, these assumptions do not hold, and inversion is applied to unstacked traces—prestack. Before discussing prestack situations in detail, we continue with the simpler case of poststack inversion.

A stacked trace is compared with the synthetic trace computed from the reflectivity model and wavelet. The differences between the two traces are used to modify the reflectivity model so that the next iteration of the synthetic trace more closely resembles the stacked trace. This process continues, repeating the generation of a synthetic trace, comparison with the stacked trace, and modification of the model until the fit between the synthetic and stacked traces is optimized.

There are many ways to construct synthetic traces, and various methods may be used to determine the best fit. A common approach for determining fit is least-squares inversion, which minimizes the sum of the squares of the differences at every time sample. This inversion technique operates on a trace-by-trace basis, while others attempt to globally optimize the inversion of the seismic volume. We discuss global optimization later.

In the simplest case, inversion produces a model of relative reflectivity at every time sample, which can be inverted to yield relative acoustic impedance. To obtain formation properties such as velocity and density, a conversion to absolute acoustic impedance is necessary. However, such a conversion requires frequencies down to near 0 Hz, lower than contained in conventional seismic data. An absolute acoustic impedance model can be constructed by combining the relative acoustic impedance model obtained from the seismic frequency range with a low-frequency model derived from borehole data (above right).

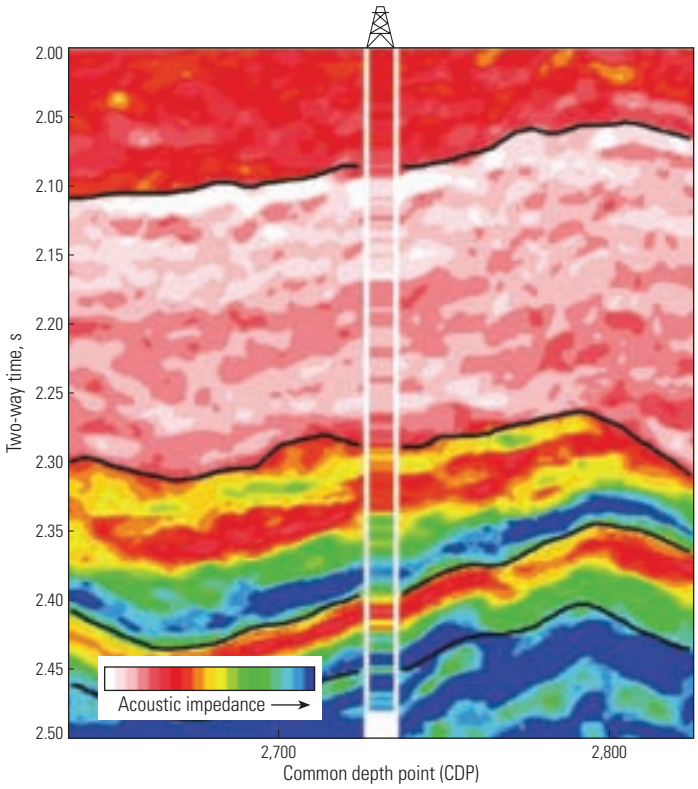

^ Absolute acoustic impedance from poststack inversion. Inversion of seismic amplitudes generated the color-coded panel, with low acoustic impedance in pink and red, and high acoustic impedance in blue and green. The acoustic impedance calculated from density and sonic logs, displayed at the well location in the middle of the panel, shows a good correlation with the seismically derived values.

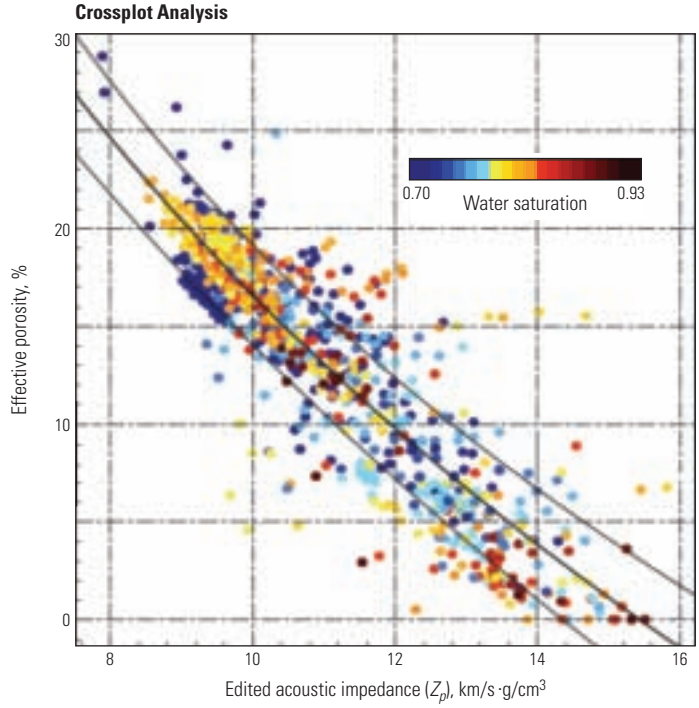

^ Acoustic impedance and porosity. The strong correlation between porosity and acoustic impedance from logs and core data in the Jsa formation indicates a robust transform for application to seismic inversion results. As in other carbonate rocks, an increase in acoustic impedance is related to a decrease in porosity. A separate porosity-acoustic impedance function was created for the Kti formation.

Relating seismically derived acoustic impedances to formation properties makes use of correlations between logging measurements. For example, crossplotting acoustic impedance and porosity measured in nearby wells establishes a transform that allows seismically measured acoustic impedance to be converted to porosity values throughout the seismic volume. An example from a carbonate reservoir in Mexico demonstrates the power of this technique.

Inversion for Porosity in Mexico

Following the 2003 discovery of the Lobina field offshore Mexico, Pemex contracted with WesternGeco to obtain a seismic survey with better resolution than one acquired in 1996. Seismic data with increased frequency content would significantly enhance the ability of interpreters to map key reservoir layers. The company's objective was to identify high-porosity zones within two carbonate layers: the primary Jurassic San Andres (Jsa) limestone and the inferior shallower Cretaceous Tamaulipas (Kti) carbonate target.

A Q-Marine high-resolution 3D seismic survey achieved a maximum frequency of 60 Hz, doubling that of the 1996 survey.[5] Inversion of the new data generated porosity maps that helped rank previously defined drilling locations, determine new potential locations and optimize development drilling.

Trace-by-trace inversion of the stacked seismic data allowed geophysicists to obtain relative acoustic impedance at every trace throughout the seismic volume. Key horizons that had been interpreted as strong acoustic events were converted from time to depth by correlation with formations seen in well logs. This combination of interpreted horizons and values of acoustic impedance at these points enabled the creation of a low-frequency model to convert the relative acoustic impedance to an absolute measurement (above left).[6]

Crossplotting porosity with acoustic impedance from logs and core data in the survey area revealed a strong correlation between the two properties—an increase in porosity causes a decrease in velocity, a decrease in density, and therefore a corresponding decrease in acoustic impedance (left). Porosity-acoustic impedance functions were created for the Jsa and Kti formations separately. Applying these correlations to the seismically derived acoustic impedance volume, geophysicists created fieldwide maps of porosity. The seismic porosity results were

checked using "blind wells," that is, wells that were not used in the inversion. The seismically derived porosity closely matched the blind-well porosity logs, adding confidence to the seismically calculated results.

The porosity maps had a significant impact on defining infill drilling locations. In the nearby Arenque field, covered by the same survey, Pemex upgraded four previously identified prospects. Increased priority was given to the two locations corresponding to higher porosity in the seismic volume. In one area, the inversion calculations allowed identification of undrilled, discrete porosity features (right). With these results, well placement could be designed to maximize contact with high-porosity zones in the Jsa formation.

In another area where seismic porosity results were used to guide drilling, a well produced oil from the Jsa formation at 2,000 bbl/d [318 m^3/d]. The seismically derived results show excellent correlation with the porosity measured in the well (below right).

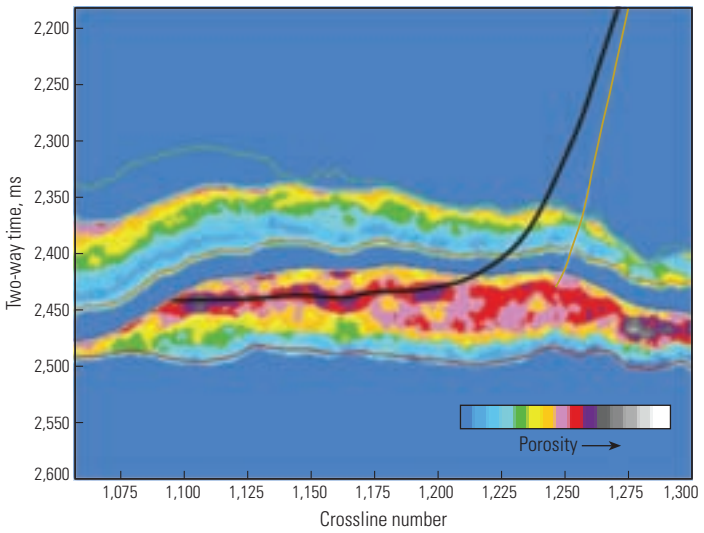

^ Identifying undrilled high-porosity targets. Inversion revealed a high-porosity interval (purple and red), helping Pemex delineate zones that could be reached with new wells. The black line is a possible well trajectory. An existing well is shown in gold.

Inversion When Offset Matters

In many cases, the stacking process does not adequately preserve amplitude. For example, when traces exhibit amplitude variation with offset (AVO), the trace that results from stacking does not have the same amplitudes as the vertical-incidence, or zero-offset, trace. Under these conditions, inversion should be performed on data that have not been stacked. Moreover, the parameters that cause the amplitude to change can be modeled and used to further the inversion process.

Data preparation for inversion of AVO traces requires steps similar to those for preparation for stacking. Traces reflecting at a common midpoint are gathered and sorted by offset, which is related to incidence angle. Then, a velocity model is applied to each gather to flatten events

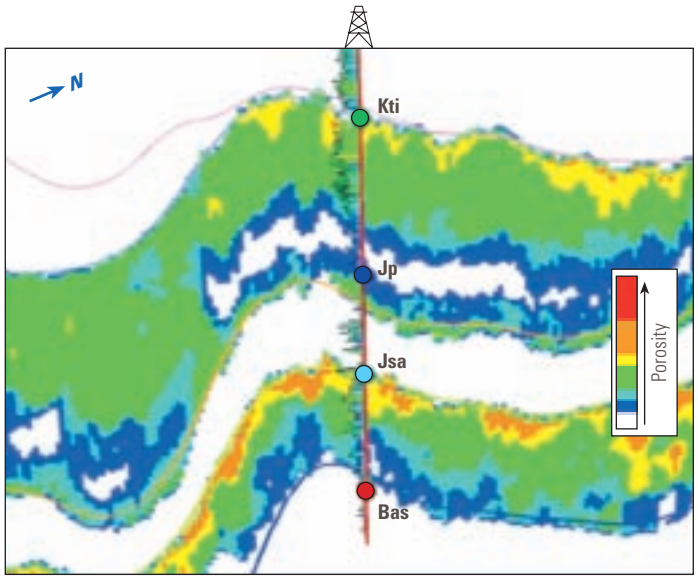

^ Results of drilling into a zone predicted to have high porosity. A well penetrated both the Cretaceous (Kti) and Jurassic (Jsa) reservoirs, encountering porosities that matched values predicted for the two carbonate zones. The green circle marks the top of the Kti formation, and the light blue circle marks the top of the Jsa formation. The porosity log, projected on the well path, has the same color-coding as the seismically predicted porosities.

5. Salter R, Shelander D, Beller M, Flack B, Gillespie D, Moldoveanu N, Gonzalez Pineda F and Camara Alfaro J: "Using High-Resolution Seismic for Carbonate Reservoir Description," *World Oil* 227, no. 3 (March 2006): 57–66.
6. Salter R, Shelander D, Beller M, Flack B, Gillespie D, Moldoveanu N, Pineda F and Camara J: "The Impact of High-Resolution Seismic Data on Carbonate Reservoir Description, Offshore Mexico," *Expanded Abstracts*, 75th SEG Annual International Meeting and Exposition, Houston (November 6–11, 2005): 1347–1350.

Single-Layer Geometry: Direct Relationship Between θ and Offset

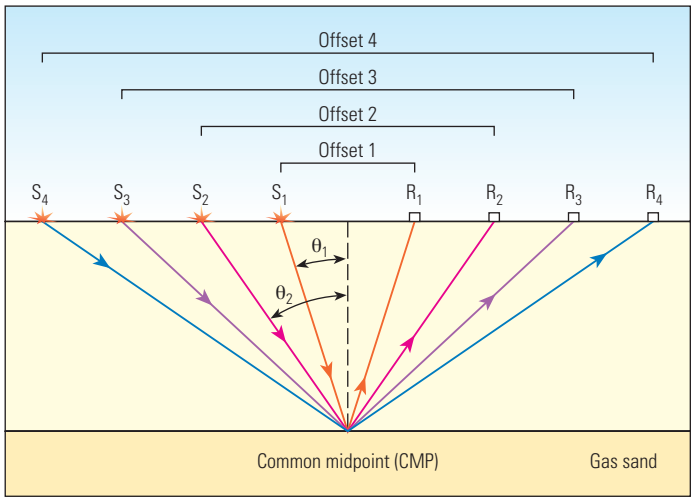

Synthetic Traces: CMP Gather

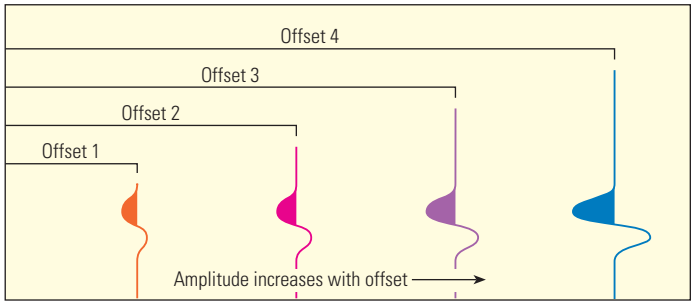

Multilayer Geometry: Complex Relationship Between θ and Offset

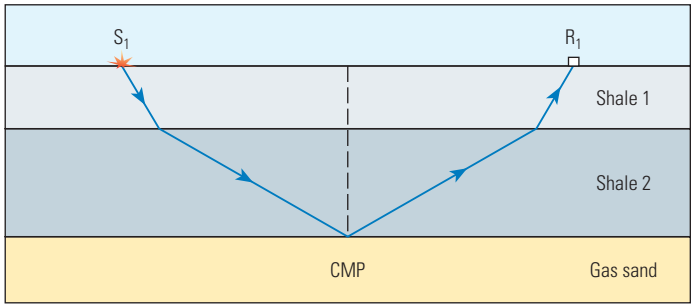

^ Amplitude variation with offset (AVO). In steps similar to preparation for stacking, traces reflecting at a common midpoint are gathered and sorted by offset (*top*), then the arrivals are flattened using a normal moveout velocity model while preserving the amplitude information (*middle*). Clearly, in this case, averaging the four traces would produce a trace that does not resemble the zero-offset trace; in other words, stacking would not preserve amplitudes. The offset versus angle (θ) relationship is determined by ray tracing (*bottom*).

to a common arrival time over all offsets (above). For a given reflection, amplitudes are tracked and plotted against offset. The flattened gather and the amplitude variation with offset comprise the data that will be compared with synthetics during the inversion process.

Most AVO inversion algorithms are based on the relationship between reflection amplitude and angle of incidence. Therefore, additional steps before inversion include converting the offset values to angles. The traces are initially labeled by source-receiver offset. The relationship between angle and offset is calculated by tracing a ray from source to receiver in an accurate velocity model.

To facilitate inversion, an AVO dataset may be divided into subsets according to angle. For example, the near-offset, mid-offset and far-offset traces may form three separate datasets. For each CMP gather, the near-offset traces are stacked and then collected with the near-offset traces from all the other CMPs, forming a near-offset dataset. Similarly, the mid-offset and far-offset traces from each CMP gather can be grouped. Each offset group can be inverted separately. Although some of the AVO information is lost in these partial stacks, sometimes called offset or angle stacks, in many cases enough remains to obtain reasonable inversion results.

Inversion of traces with AVO is more complicated than poststack inversion because the reflectivity formula is more elaborate, with dependence not only on density and compressional velocity, but also on shear velocity and angle of incidence. The general expressions for the angular dependence of the reflection of compressional and shear waves as functions of densities, velocities and incident angle are known as the Zoeppritz equations.[7] Because the full Zoeppritz formulation is cumbersome, approximations are often used to generate synthetics and facilitate fast inversion.[8]

Each approximation method attempts to fit a simplified formula to the curve of reflection amplitude versus angle of incidence (next page, top right). The simplified approaches differ in the number of terms used in the approximation—usually two or three—and in the parameters solved for. Some two-parameter inversions calculate *P*-wave impedance (Z_p, equal to ρV_p) and *S*-wave impedance (Z_s, equal to ρV_s). A three-parameter inversion might determine Z_p, Z_s and density (ρ), but a three-parameter inversion for Z_p, V_p/V_s and ρ would contain the same information. Some approximations are expressed in terms of Poisson's ratio (ν), shear modulus (μ), bulk modulus (λ) and ρ, which again are related to V_p and V_s.

The number of parameters that can be solved for depends on the range of offsets—or equivalently, angles—available and on data quality. If a large range of offsets or angles is available and the signal-to-noise ratio at high offset is good, three parameters may be resolved. If offsets are limited, then inversion may deliver only two parameters reliably. Density is the most difficult parameter to invert for; the process requires long offsets and high-quality data.

A case study presents three-parameter inversion on AVO data acquired offshore Egypt.

Inversion in the Nile Delta

Apache Egypt Companies, with partners RWE Dea and BP Egypt, recorded a 3D seismic survey in a western Mediterranean deep marine concession in the Nile Delta.[9] The seismic data exhibited strong amplitudes over a gas-charged complex of channel and levee sands. However, amplitude alone was not a reliable indicator of gas saturation: distinct accumulations—one with high gas saturation and the other with low gas saturation—both displayed high amplitude. Extracting density information from the seismic data was a key to identifying commercial gas sands.

The main objective of prestack inversion was to improve the existing reservoir model in preparation for optimizing the appraisal and development plan. The survey featured long offsets, up to 6,000 m [19,690 ft], enabling AVO inversion for three elastic parameters: *P*-wave impedance, *S*-wave impedance and density. Correlation with log data would help Apache estimate rock and fluid properties throughout the 1,500-km^2 [580-mi^2] study area.

Rock-property correlations using log data from the five wells in the concession discriminated rock-fluid classes on the basis of V_p/V_s and *P*-wave impedance (below right). The separation between sands with high and low water saturations suggested that fluid-content differences would be apparent in the inversion results.

	V_p	V_s	ρ	R_0	V_p/V_s	Poisson's Ratio
Layer 1	2,800	1,700	2.3		1.647059	0.208081
Layer 2	3,000	2,000	2.2	0.01227	1.5	0.1

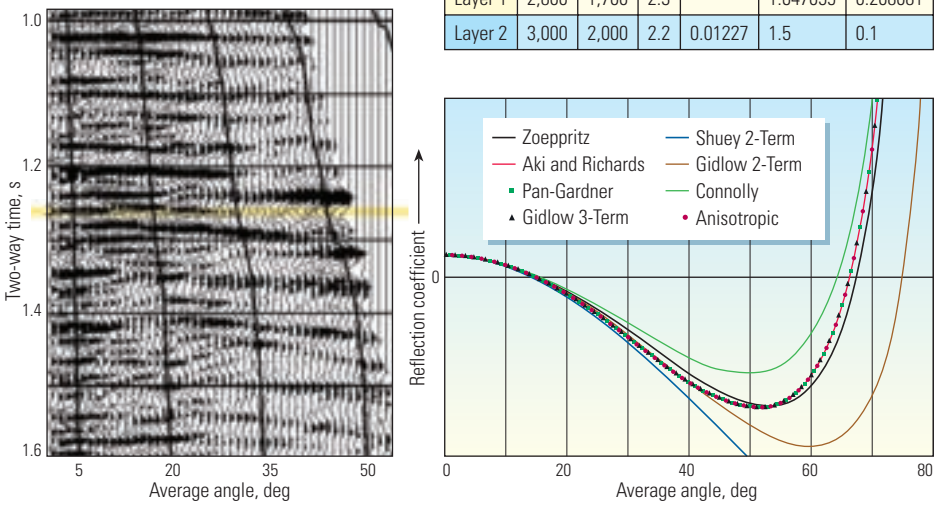

^ Amplitude variation with offset data and reflection coefficient versus angle of incidence. Several reflections in the CMP gather (*left*) exhibit amplitude variation with offset. These data come from the North Sea example described on page 51. The nearly vertical black lines delimit angle ranges computed by ray tracing. The reflection of interest is at 1.26 s (yellow). At zero offset (normal incidence), the reflection has slightly positive amplitude—a swing to the right—then turns negative, with a swing to the left. Several methods can be used to model the reflection coefficient versus angle (*right*). The properties of the two-layer model are shown (*top*). R_0 stands for reflection coefficient at zero offset. The exact solution by the Zoeppritz equations is shown by the black curve. The other curves are approximations taken from the work described in reference 8.

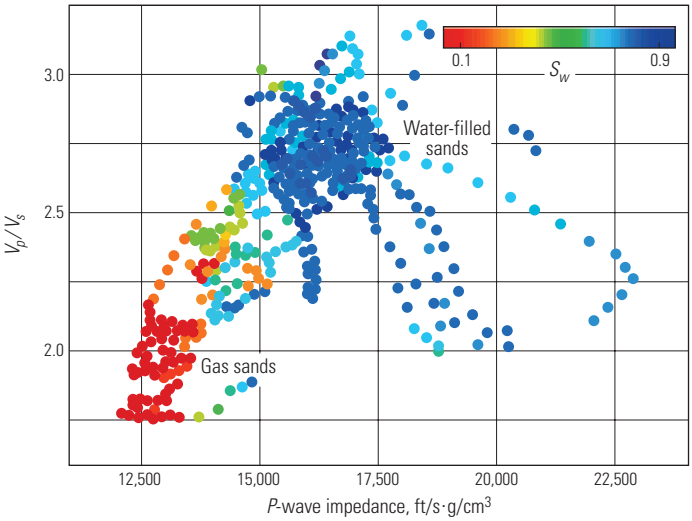

^ Correlating acoustic properties with water saturation (S_w). Log measurements of *P*-wave impedance, water saturation and V_p/V_s are crossplotted to show relationships that can be applied to seismic inversion results. Clean gas sands are plotted in red, laminated sands in green, and water-filled sands in blue. (Adapted from Roberts et al, reference 9.)

7. Zoeppritz K: "Über Erdbebenwellen, VIIB: Über Reflexion und Durchgang seismicher Wellen durch Unstetigkeitsflächen," *Nachrichten der Königlichen Gesellschaft der Wissenschaften zu Göttingen, Mathematisch-physikalische Klasse* (1919): 57–84.
8. Aki K and Richards PG: *Quantitative Seismology: Theory and Methods*. San Francisco: W.H. Freeman and Company, 1980.
   Connolly P: "Elastic Impedance," *The Leading Edge* 18, no. 4 (April 1999): 438–452.
   Pan ND and Gardner GF: "The Basic Equations of Plane Elastic Wave Reflection and Scattering Applied to AVO Analysis," Report S-87-7, Seismic Acoustic Laboratory, University of Houston, 1987.
   Rüger A: "*P*-Wave Reflection Coefficients for Transversely Isotropic Models with Vertical and Horizontal Axis of Symmetry," *Geophysics* 62, no. 3 (May–June 1997): 713–722.
   Shuey RT: "A Simplification of the Zoeppritz Equations," *Geophysics* 50, no. 4 (April 1985): 609–614.
   Smith GC and Gidlow PM: "Weighted Stacking for Rock Property Estimation and Detection of Gas," *Geophysical Prospecting* 35, no. 9 (November 1987): 993–1014.
9. Roberts R, Bedingfield J, Phelps D, Lau A, Godfrey B, Volterrani S, Engelmark F and Hughes K: "Hybrid Inversion Techniques Used to Derive Key Elastic Parameters: A Case Study from the Nile Delta," *The Leading Edge* 24, no. 1 (January 2005): 86–92.

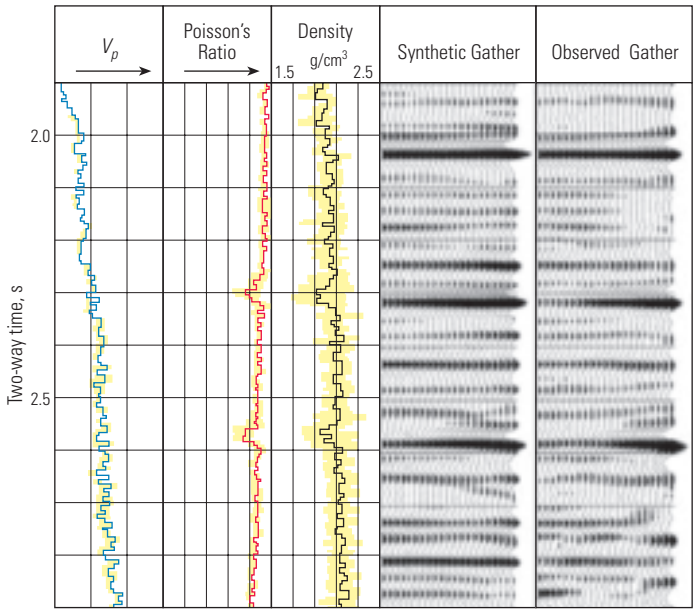

^ Comparison between observed and synthetic AVO gathers. The observed AVO gather (*right*) was inverted for V_p, Poisson's ratio and density. The results (left three panels) are plotted with associated uncertainty range (yellow). A synthetic gather generated from the V_p, Poisson's ratio and density models appears in the fourth panel. The close match between the observed and synthetic AVO gathers indicates that the property models are good representations of actual earth properties. (Adapted from Roberts et al, reference 9.)

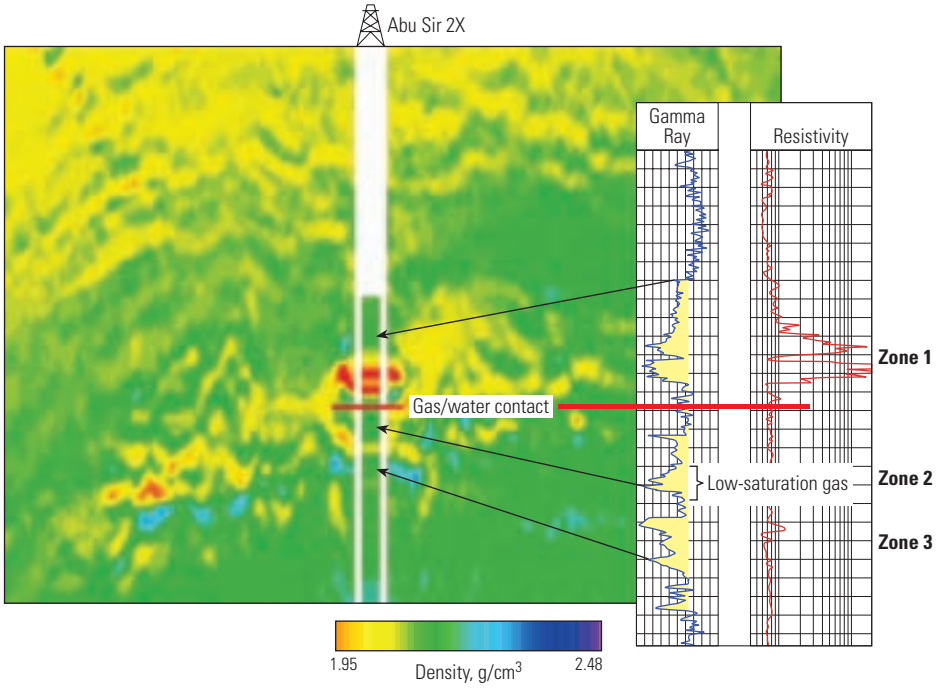

^ Inversion for density. Inversion of AVO data over gas fields in the Nile Delta predicts low density (red) in the upper part of the reservoir (Zone 1) and higher densities (green and yellow) deeper in the reservoir (Zones 2 and 3). The density measured at the well location is inserted in the center of the panel and plotted on the same color scale as the seismic-inversion density. The well logs (*inset right*) show where sands were logged (yellow shaded gamma ray) and where high resistivity (red curve) indicates hydrocarbon. The seismic amplitude section, not shown, exhibited high amplitudes in all zones of the reservoir, and so was unable to distinguish the low gas saturation in Zones 2 and 3 from the high gas saturation of Zone 1. (Adapted from Roberts et al, reference 9.)

The inversion workflow combined full-waveform prestack inversion with three-term AVO inversion. The prestack inversion, performed at sparsely sampled locations, provided background V_p/V_s trends, which, with the well data, were used to build low-frequency models to merge with the results of the AVO inversion. Agreement between synthetic predictions and actual results was generally good (left).

The three-parameter AVO inversion results were converted into relative impedances and merged with the low-frequency background models to generate 3D volumes of *P*-wave impedance, *S*-wave impedance and density. With transforms derived from rock-physics analysis, these elastic attributes were then converted to volumes of net-to-gross sand and bulk water saturation.

The density volume was found to be a reliable indicator of fluid saturation. For example, the Abu Sir 2X well, drilled at a location of high seismic amplitudes, encountered one zone with high gas saturation and two deeper zones with low gas saturation (below left). A seismically derived density profile through the well predicts low gas saturation in the deeper layers. The density results from seismic inversion delineate a single high-saturation interval and also show its limited lateral extent.

The inversion results can be examined from a variety of perspectives. For instance, tracking one of the layers that was uneconomic in the Abu Sir 2X well throughout the seismic volume reveals a region where that layer might contain high gas saturation (next page, bottom). Although this accumulation is downdip from the reservoir encountered in other wells in the area, the density and water-saturation maps support the interpretation that the downdip area has high gas saturation and is not water-filled. As a consequence of this study, a new well, Abu Sir 3X, is planned for this area.

10. For more on drilling injectite targets: Chou L, Li Q, Darquin A, Denichou J-M, Griffiths R, Hart N, McInally A, Templeton G, Omeragic D, Tribe I, Watson K and Wiig M: "Steering Toward Enhanced Production," *Oilfield Review* 17, no. 3 (Autumn 2005): 54–63.
11. Pickering S and McHugo S: "Reservoirs Come in All Shapes and Sizes, and Some Are More Difficult Than Others," *GEO ExPro* no. 1 (June 2004): 34–36.
McHugo S, Cooke A and Pickering S: "Description of a Highly Complex Reservoir Using Single Sensor Seismic Acquisition," paper SPE 83965, presented at SPE Offshore Europe, Aberdeen, September 2–5, 2003.

Inversion to Enhance Visibility

In some cases, the acoustic impedance contrast between two lithologies may be so small that the interface between them generates almost no normal-incidence reflection. For example, an oil-filled sandstone with high density and low *P*-wave velocity might have nearly the same acoustic impedance as a shale with lower density and higher *P*-wave velocity. Without an acoustic impedance contrast, such oil reservoirs are extremely difficult to detect using traditional surface seismic acquisition and processing.

An example of a low-contrast reservoir is the Alba field in the North Sea. Alba and reservoirs like it are interpreted to be injectites, formed by the injection, or remobilization, of unconsolidated sand into overlying shale layers during periods of differential stress (above right). These complex reservoirs are characterized by irregular morphology and chaotically distributed high-porosity sands. Often, such accumulations are not discovered by seismic imaging, but are encountered inadvertently while drilling to deeper targets.[10]

In one area of the central North Sea, an operating company wanted to improve the seismic characterization of injected reservoir sands in the Balder interval that were particularly difficult to image.[11] Modeling studies using rock properties from well data established that prestack inversion of seismic data could

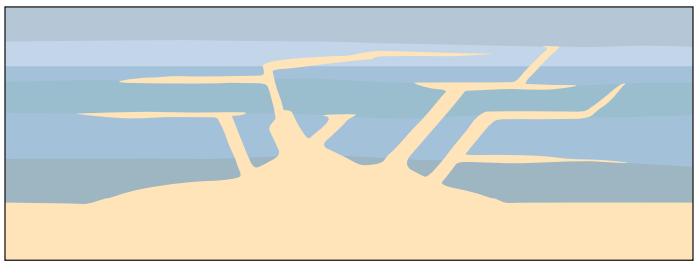

^ Sand-injection features, or injectites. The remobilization of unconsolidated sand (gold) into overlying shale layers (gray) can result in injectites. These sandstone features have irregular shapes and are difficult to image seismically.

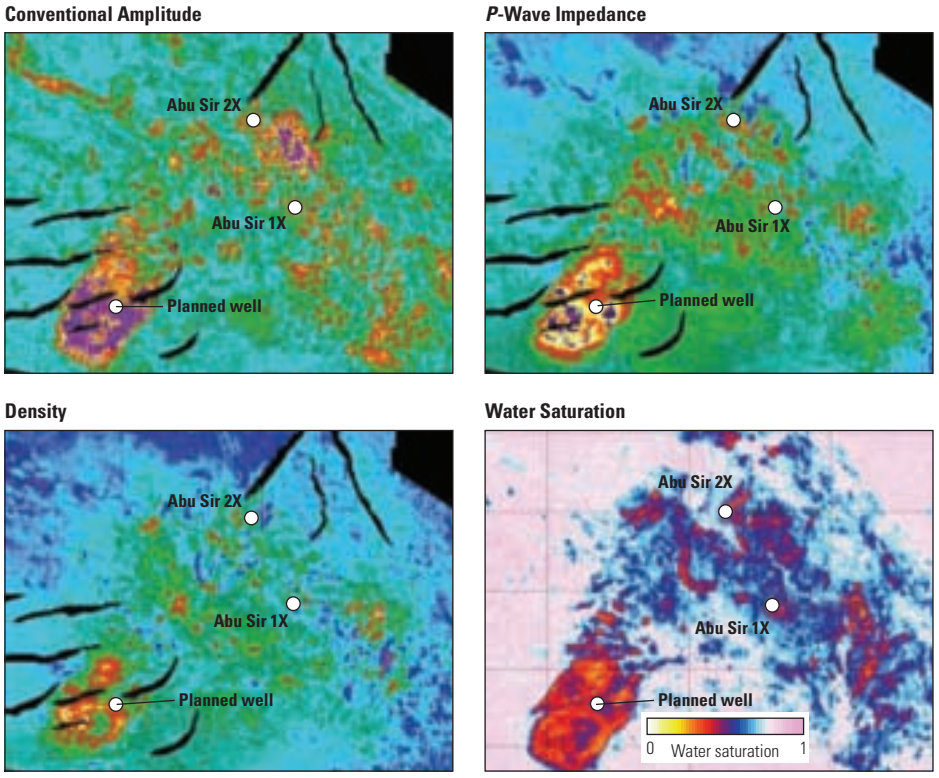

^ Tracking inversion results through the reservoir. Parameters extracted from the seismic data and its inversion are displayed for Zone 2—one of the zones that had uneconomic gas saturations in the Abu Sir 2X well. The amplitudes of the original seismic data (*top left*) show anomalies near the Abu Sir 2X well, but the density plot (*bottom left*) does not. Low amplitudes are plotted in blue and green, and high amplitudes are plotted in red and purple. Low densities are plotted in red and high densities are plotted in blue and green. Amplitude, density and *P*-wave impedance (*top right*) all exhibit exceptional values in the southeast corner, where a well is planned. Low P-wave impedances are plotted in red and purple, and high impedances are plotted in blue and green. Conversion of the inversion results to water saturation (*bottom right*) indicates that the planned well should encounter low water saturation. (Adapted from Roberts et al, reference 9.)

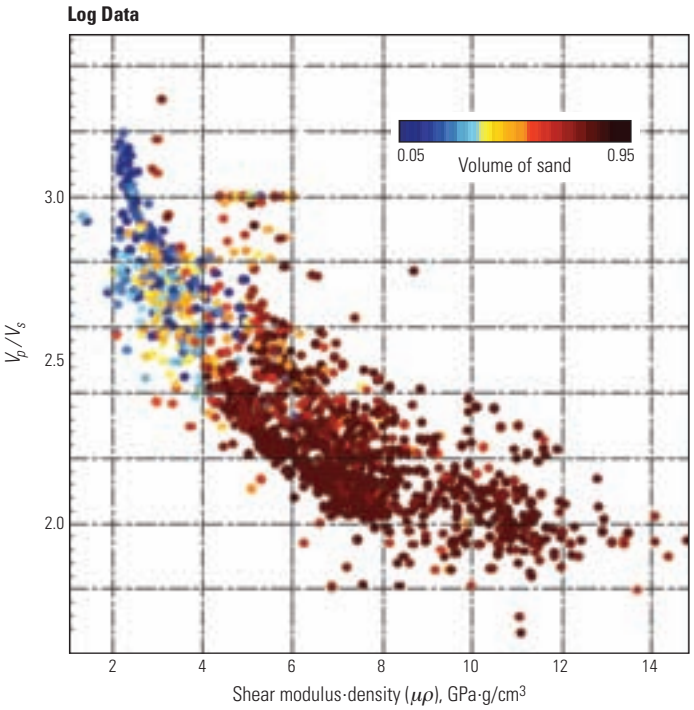

^ Correlating acoustic properties with lithology. A crossplot of V_p/V_s with the product of shear modulus (μ) and density (ρ) shows a trend related to sand volume: high sand content correlates with low V_p/V_s and high $\mu\rho$ values. Applying this relation to V_p/V_s and $\mu\rho$ values obtained from inversion yields lithology maps of the subsurface.

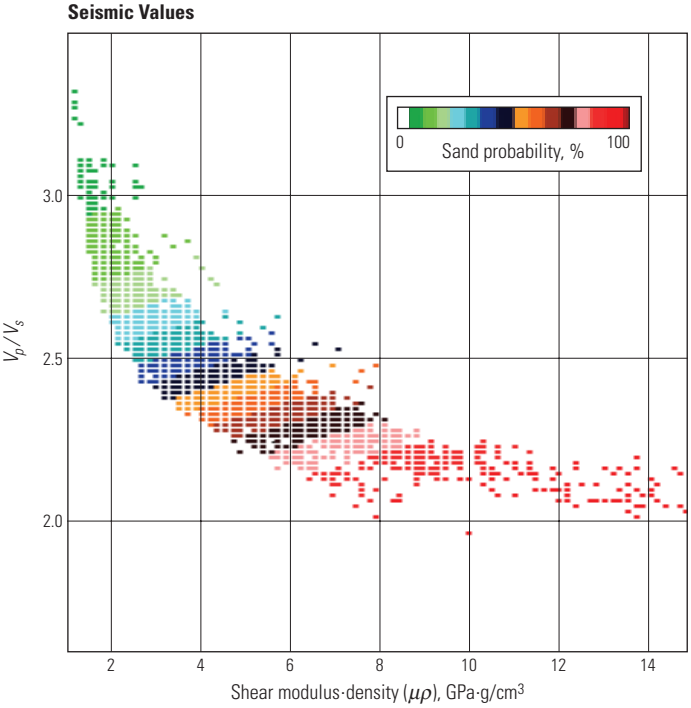

^ Sand probability. The correlation between inversion outputs V_p/V_s and $\mu\rho$ with sand probability shows a direct relationship: increasing $\mu\rho$ and decreasing V_p/V_s point to higher probability of sand. This relationship was applied to the seismic inversion results to obtain maps of sand probability.

potentially distinguish the clean sands from the surrounding shales, but the existing surface seismic data were of insufficient resolution for this purpose.

A new survey was designed to map the distribution and thickness of reservoir pay, delineate the geometry of individual sand wings and assess reservoir connectivity. Acquisition with the Q-Marine system would allow accurate cable positioning, fine spatial sampling and calibration of sources and receivers. Together, these capabilities facilitate precision imaging, improved noise attenuation, increased bandwidth and preservation of amplitude and phase information—all important for successful inversion.

Log data from three wells intersecting the reservoir were analyzed for correlations between *P*- and *S*-wave velocities, ρ, μ, λ, lithology and fluid saturation. For example, crossplotting V_p/V_s with the product $\mu\rho$, and color-coding by lithology, showed that high sand content correlated with low V_p/V_s and high $\mu\rho$ values (left). These relationships were then applied to V_p/V_s calculated from seismic inversion to map high sand content throughout the seismic volume.

The prestack seismic data were divided into seven angle stacks, each containing reflections in a 7° range of incidence angles out to 49° (next page, bottom). Three-parameter AVO inversion generated estimates of *P*- and *S*-wave reflectivities and density contrast. These volumes were inverted for *P*- and *S*-wave impedances and density, from which volumes of $\mu\rho$, V_p/V_s and λ/μ were generated.

Crossplots of seismically derived V_p/V_s and $\mu\rho$ through the interval containing the injected sands were color-coded by sand probability (left). Applying the color-coding to the rock-constant volumes obtained from seismic inversion yielded interpretable 3D cubes of sand probability. A close-up of a section through the sand-probability volume highlights a steeply dipping sand-injection feature (next page, top).

The sand-probability volume can be illuminated by rendering the surrounding shales—lithologies with low probability of

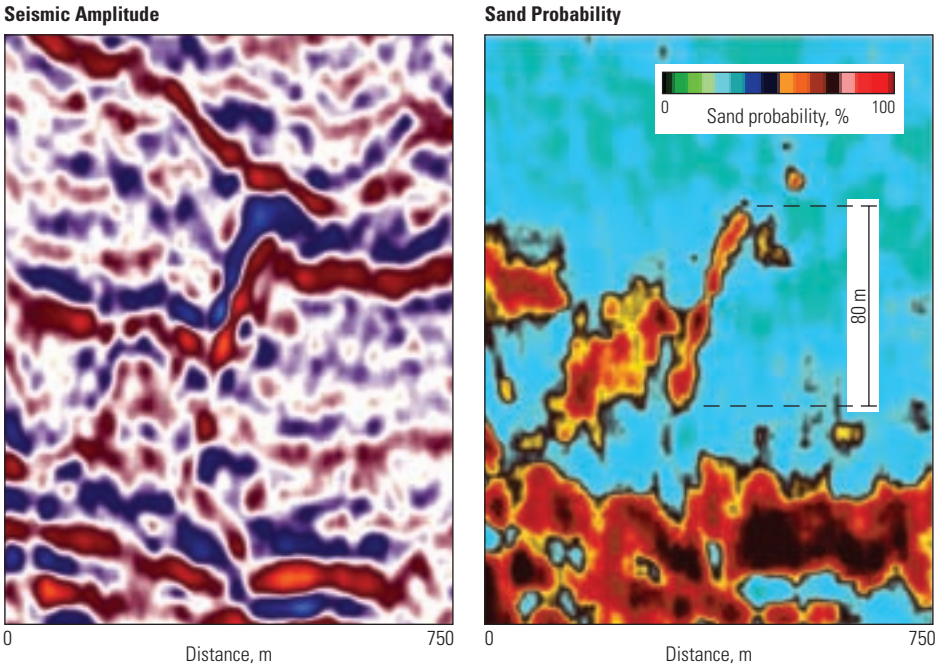

^ Comparing seismic reflection amplitudes with sand probability. A steeply dipping feature seen in the center of the seismic reflection image (*left*) has a high probability of being sand (*right*). This structure, which is 80 m [260 ft] high, has the shape and aspect expected of a sand injectite.

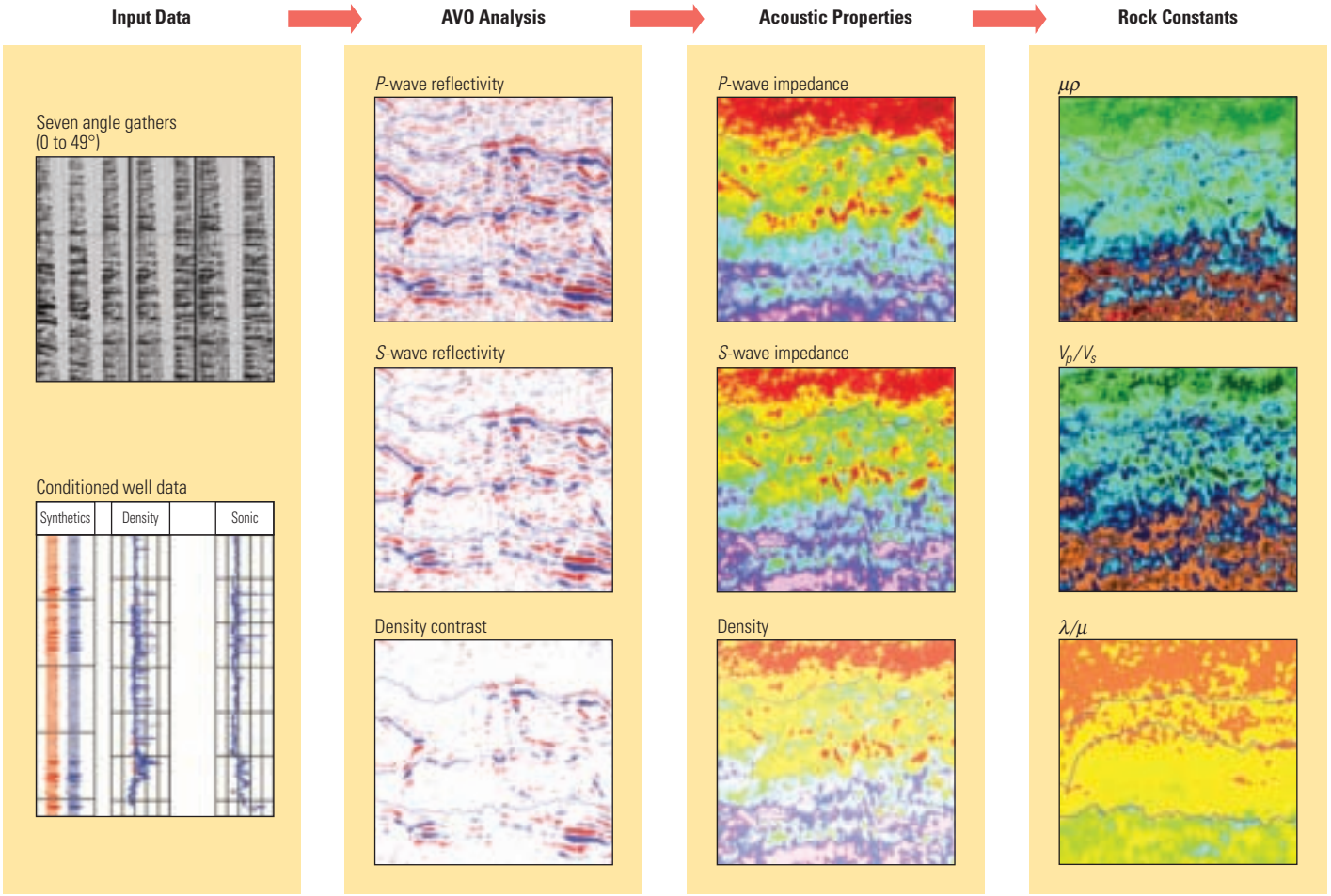

^ AVO inversion workflow. The input data consisted of prestack AVO gathers in 7° offset ranges, along with sonic and density well logs (*left*). The first step, three-parameter AVO inversion, produced estimates of *P*-wave and *S*-wave reflectivities and density contrast. These volumes were inverted for *P*-wave and *S*-wave impedances and density. The final step extracted rock properties, in the form of $\mu\rho$, V_p/V_s and λ/μ.

Sand-Intrusion Visualization

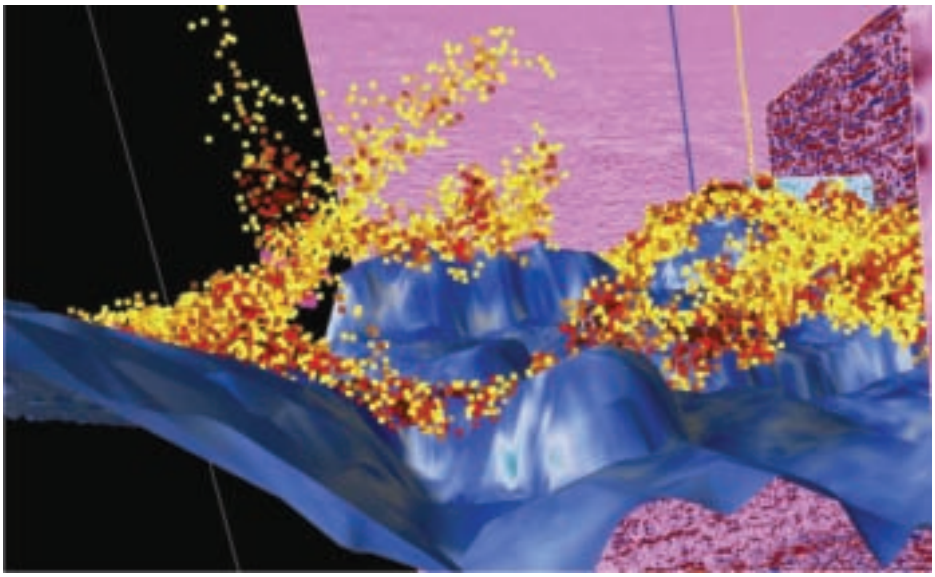

^ Seeing the sand. Volumes with high sand probability are colored yellow, gold and red, and the portions with low probability of sand have been made transparent. The top surface of the underlying sand formation from which the injectite was ejected is blue. (Adapted from Pickering and McHugo, reference 11.)

sand—transparent using 3D visualization technology (above). This characterization of the extent and quality of the injected sand bodies can help optimize development of these complex features.

Simultaneous Inversion

The examples presented so far have shown the results of techniques that invert traces separately and then combine the results in a display of reflectivity. Geophysicists at the Danish company Ødegaard, now part of Schlumberger, have developed a simultaneous inversion technique that examines all traces at once to invert for a globally optimized model of rock properties.[12]

Global optimization is a term describing several methods designed to find the best overall solution of a problem that has multiple local solutions. An inversion problem may be cast as finding the absolute minimum of a multidimensional, nonlinear function (right). This can be likened to placing a ball on a hilly surface and letting it roll to the lowest level. Depending on which hill the ball starts on and which direction it rolls, it may get stuck in a nearby low spot—a local minimum—or land in the lowest area in the space—the global minimum.

Analogously, some inversion techniques depend heavily on the starting model—which hill they start on—and so may find a local minimum rather than the absolute minimum. Global optimization attempts to find the absolute minimum by adopting new ways of searching for solution candidates. Various strategies may be utilized to reach a solution. The approach taken by the ISIS suite of reservoir characterization technology developed by Ødegaard is simulated annealing.

Simulated annealing is based on a physical analogy. In metallurgy, annealing is the process of controlled heating and subsequent cooling of a metal. Heating increases the internal energy of the metal atoms, causing them to abandon their places in the crystal structure. Gradual cooling allows the atoms to reach lower energy states. Under properly controlled heating and cooling, the system becomes more ordered; crystal size increases, and the resulting material has minimal defects.

Instead of minimizing the thermodynamic energy of a system, inversion by simulated annealing aims to minimize an objective function, also called a cost function. The algorithm replaces the starting solution with another attempt by selecting a random solution not far from the first. If the new solution reduces the cost function, it is kept, and the process is repeated. If the new solution is not much better than the previous one, another random solution is tested. However, simulated annealing improves over some other methods by allowing a "worse" solution if it helps investigate more of the solution space.

The ISIS simultaneous inversion cost function is made up of four penalty terms that are collectively minimized to deliver the best solution. The first term contains a penalty for differences between the seismic data and the synthetic. The second term includes the low-frequency acoustic impedance trend in the inversion through a penalty for deviation of the estimated acoustic impedance model from the low-frequency model. The third term attenuates horizontally uncorrelated noise by introducing a penalty for horizontal variations in the estimated acoustic impedance model. The fourth term introduces a sparsely parameterized background model of layer boundaries. These terms can be modified to include requirements of more complex data types, such as time-lapse surveys and shear waves.

Compared with trace-by-trace reflectivity methods, simultaneous inversion has several benefits. Honoring the full bandwidth of the seismic signal—low and high frequencies together—enhances resolution and accuracy.

The ISIS inversion algorithm can be used on many types of seismic data (next page, top right). The remainder of the article focuses on three distinct applications: a 3D AVO study from Australia, a time-lapse example from the North Sea and a multicomponent case using seabottom sensors also from the North Sea.

Revealing a Reservoir in Australia

Many seismic surveys are acquired and processed purely for reflector-imaging purposes, without inversion in mind. However, inversion

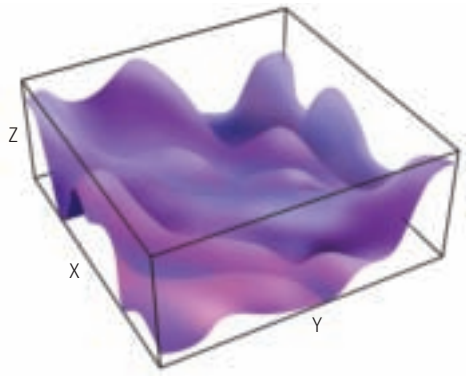

^ Finding the minimum. Many inversion schemes attempt to minimize a multidimensional, nonlinear cost function with multiple minima. In this case, the minima are shown as low points in this 3D surface. Depending on the inversion algorithm and starting point, the process might end in a local minimum—the point that is the lowest in a neighborhood—instead of the global minimum—the lowest point of all.

can deliver even better results when survey design, acquisition and processing are tailored to the requirements of the inversion scheme.

Operating offshore Western Australia, Santos Ltd. and partners wanted to enhance recovery from their reservoir, and accurate mapping would help achieve this.[13] However, even after reprocessing, the seismic data acquired in 1998 were not of sufficient quality to allow interpretation of the top and base of the primary reservoir.[14]

Rock-physics analysis of well logs revealed that the contrast in *P*-wave impedance between the reservoir and the overlying shale was subtle. This explained some of the difficulty in identifying the reservoir in vertical-incidence reflection data. However, a large contrast in Poisson's ratio should be observable if AVO data in the appropriate offset range were acquired.

In addition to the low-reflectivity problem, the 1998 survey data were noisy. The continental shelf offshore northwest Australia has a layer of high acoustic impedance contrast near the seafloor. This layer traps seismic energy, generating reverberations called multiples that contaminate the seismic record.

WesternGeco survey evaluation and design (SED) specialists investigated ways to eliminate noise and improve overall recording in a new survey. Removing the noise from multiples required an accurate image of the seafloor, which could be acquired if extremely short offsets were recorded. The 3.125-m [10.25-ft] spacing of Q-Marine hydrophones would adequately sample both the desired signal and the noise, facilitating effective removal of the latter. Modeling showed that a streamer length exceeding 5,000 m [16,400 ft] would be needed to capture AVO effects at the reservoir level. This length would provide data over an incidence-angle range of 10 to 50°.

Comparison of a reflection-amplitude image from the 2006 Q-Marine survey with one from the reprocessed 1998 dataset shows improved structural imaging and reduced noise (right). Testing during processing identified the steps that would optimize inversion.

12. Rasmussen KB, Brunn A and Pedersen JM: "Simultaneous Seismic Inversion," presented at the 66th EAGE Conference and Exhibition, Paris, June 7–10, 2004.
13. Partners were Kuwait Foreign Petroleum Exploration Company (KUFPEC), Nippon Oil Exploration and Woodside Energy.
14. Barclay F, Patenall R and Bunting T: "Revealing the Reservoir: Integrating Seismic Survey Design, Acquisition, Processing and Inversion to Optimize Reservoir Characterization," presented at the 19th ASEG International Geophysical Conference and Exhibition, Perth, Western Australia, November 18–22, 2007.

Data Type	Physical Properties
Full-stack data	*P*-wave impedance
Partial-stack AVO data	*P*-wave impedance, V_p/V_s (or *S*-wave impedance) and density, from which Poisson's ratio, λ and μ can be estimated.
Intercept and gradient AVO data	Acoustic impedance from the intercept data; shear impedance from shear seismic data calculated from the intercept and gradient data
Multicomponent full-stack data (*P*-to-*P* and *P*-to-*S* conversions)	*P*-wave impedance and *S*-wave impedance
Multicomponent partial-stack AVO data	*P*-wave impedance, V_p/V_s (or *S*-wave impedance) and density
Borehole seismic (VSP) data	Acoustic impedance from the *PP* data; shear impedance from the *PS* data
Time-lapse full-stack data (which may include multicomponent full-stack data)	Simultaneous time-lapse inversion for baseline *P*-wave impedance and the changes in *P*-wave impedance for each time interval: for multicomponent data, inversion will also output baseline *S*-wave impedance and changes in *S*-wave impedance over the time interval.
Time-lapse partial-stack AVO data (which may include multicomponent partial-stack AVO data)	Simultaneous time-lapse inversion for baseline properties and the changes: for example, for partial-stack data, inversion can determine baseline *P*-wave impedance, V_p/V_s (or *S*-wave impedance) and density and the changes in these properties over the time interval.

^ Applications of ISIS simultaneous inversion.

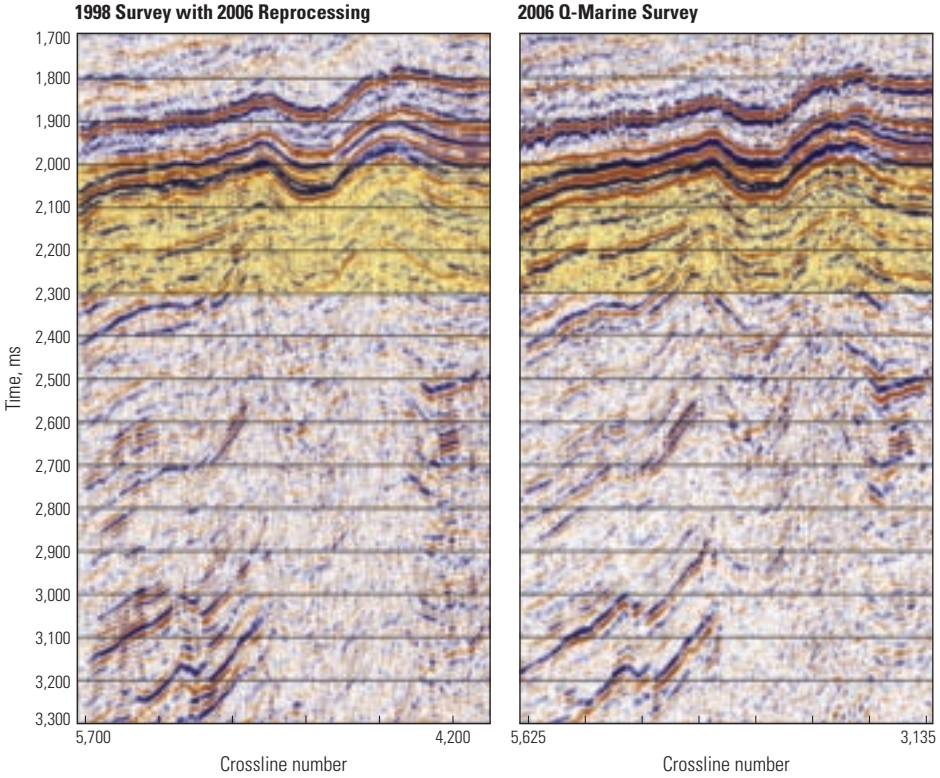

^ Seismic images in an Australian field. Multiples generated by a high acoustic impedance layer near the seafloor make it difficult to image the low-impedance-contrast reservoir, which is within the shaded interval, at approximately 2,100 to 2,200 ms. The Q-Marine image (*right*) exhibits less noise and better resolution of structural features than the 1998 dataset (*left*). (Adapted from Barclay et al, reference 14.)

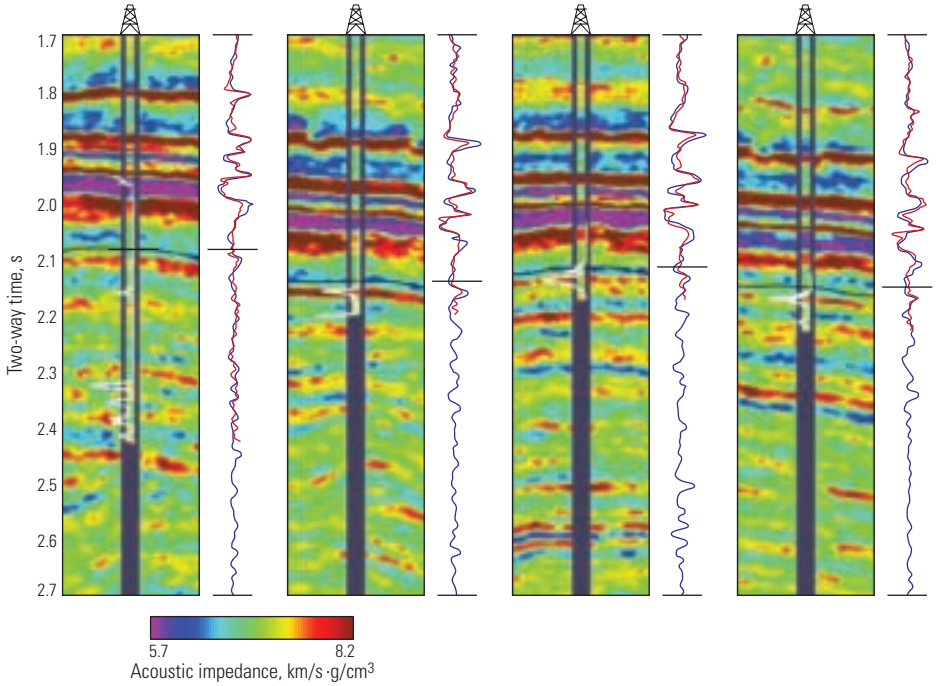

^ Simultaneous inversion for *P*-wave impedance. Impedance sections from inversion show excellent correlation with values in four wells. In each panel, the impedances measured in the well are color-coded at the same scale as the inversion results and inserted in the middle of the panel. The top of the reservoir is marked with a nearly horizontal black line. The white curves are unscaled water saturation logs, with water saturation decreasing to the left. To the right of each panel is a display of the log acoustic impedance (red) and the seismically estimated acoustic impedance at the well location (blue). (Adapted from Barclay et al, reference 14.)

The inversion for *P*-wave impedance gave high-quality results that correlated strongly with values measured in four of the field's wells (left). The subtle rise in acoustic impedance at the top of the reservoir, although significantly smaller than those in the overlying layers, is accurately detected by the simultaneous inversion.

The *P*-wave impedance contrast at the top of the reservoir is small, but the contrast in Poisson's ratio is significant, and so is a potentially more useful indicator of reservoir quality. Poisson's ratio is more accurately estimated by including large incidence angles in the inversion. A comparison of Poisson's ratio obtained by incorporating different ranges of incidence angles showed greater resolution and less noise when wider angles were included (below).

Time-Lapse Inversion

Simultaneous inversion can incorporate data from various vintages to highlight time-lapse changes in rock and fluid properties. This approach has recently been tested on the Norne field, where operator StatoilHydro is trying to increase oil recovery from 40% to more than 50%.

The Norne field has had multiple time-lapse, or 4D, seismic surveys.[15] The high-quality sandstone reservoirs, with porosities of 25 to 32%

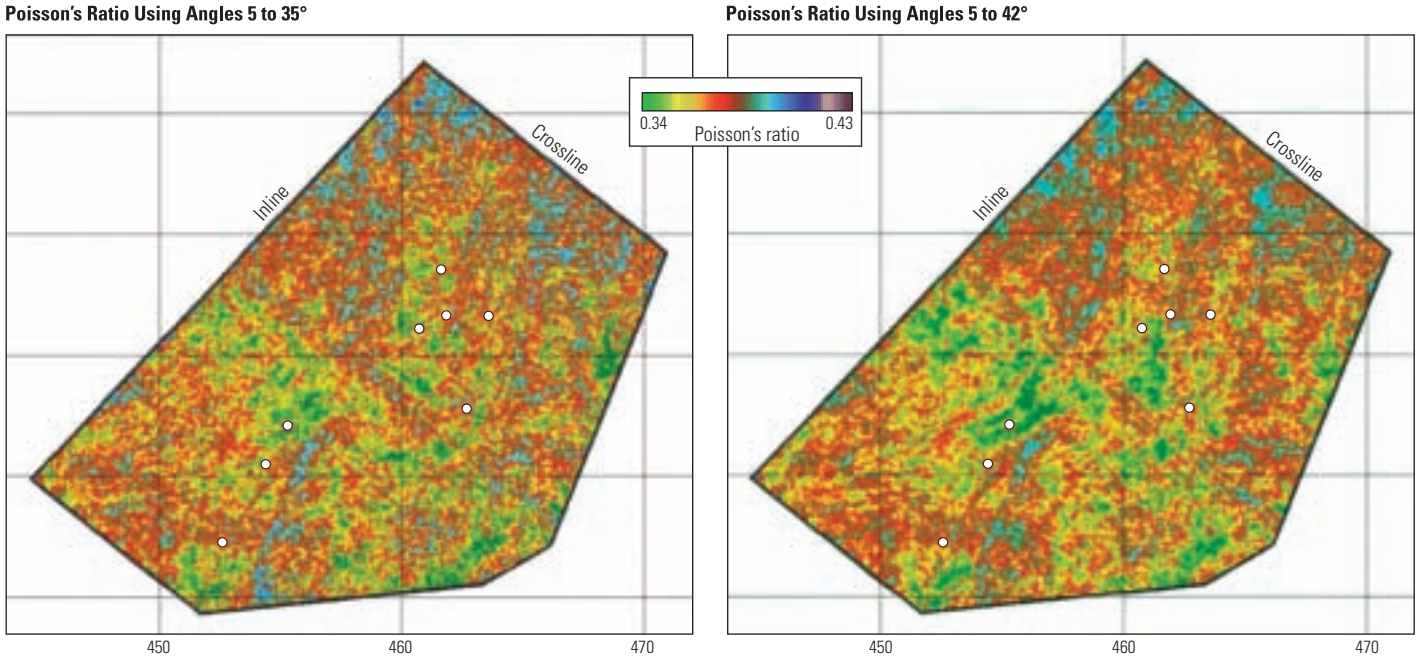

^ Inversion for Poisson's ratio. In this field, Poisson's ratio provides a better measure than acoustic impedance for assessing reservoir quality. Low Poisson's ratio (green) is generally indicative of higher quality sand. Reflection amplitudes are more affected by Poisson's ratio at larger angles of incidence. When a larger range of angles (5 to 42°) is included in the inversion (*right*), the estimation of Poisson's ratio shows less noise, and the regions of similar Poisson's ratio appear more continuous than when inversion uses a smaller range (5 to 35°) of angles (*left*). White circles are well locations. (Adapted from Barclay et al, reference 14.)

and permeabilities ranging from 200 to 2,000 mD, are conducive to successful time-lapse monitoring; changes in fluid saturation and pressure give rise to noticeable differences in seismic amplitudes and elastic impedances.

The first 3D surface seismic survey over the field was acquired in 1992. This large exploration survey was acquired before production and water and gas injection, but was not considered a baseline for time-lapse monitoring. In 2001, Norne's first Q-Marine survey was acquired, with repeatable acquisition, forming the baseline for the 2003, 2004 and 2006 monitor surveys—all acquired with Q-Marine technology.

From the start, time-lapse monitoring delivered crucial information for optimizing field development. Differences in the AVO inversions of the 2001 and 2003 surveys revealed changes in acoustic impedance that could be interpreted as increases in water saturation.[16] In one area, the trajectory of a planned well was modified to avoid a zone inferred to have high water saturation.[17]

Recently, the evaluation of changes in effective stress has become important for optimizing reservoir depletion and injection strategies. To understand the continuing effects of production on the field, StatoilHydro and Schlumberger undertook a simultaneous inversion project that incorporated all available seismic data, log data from seven wells and production data from the ECLIPSE reservoir model.[18]

The ISIS simultaneous inversion estimated baseline values and changes in acoustic impedance and Poisson's ratio from the time-lapse seismic data (right). To compensate for the lack of low-frequency information in the seismic bandwidth—needed to determine absolute elastic properties—background models were constructed. For the baseline survey, the background model was derived by propagating borehole values of elastic properties throughout the zone of interest, constrained by key interpreted horizons and the seismic velocities in each interval.

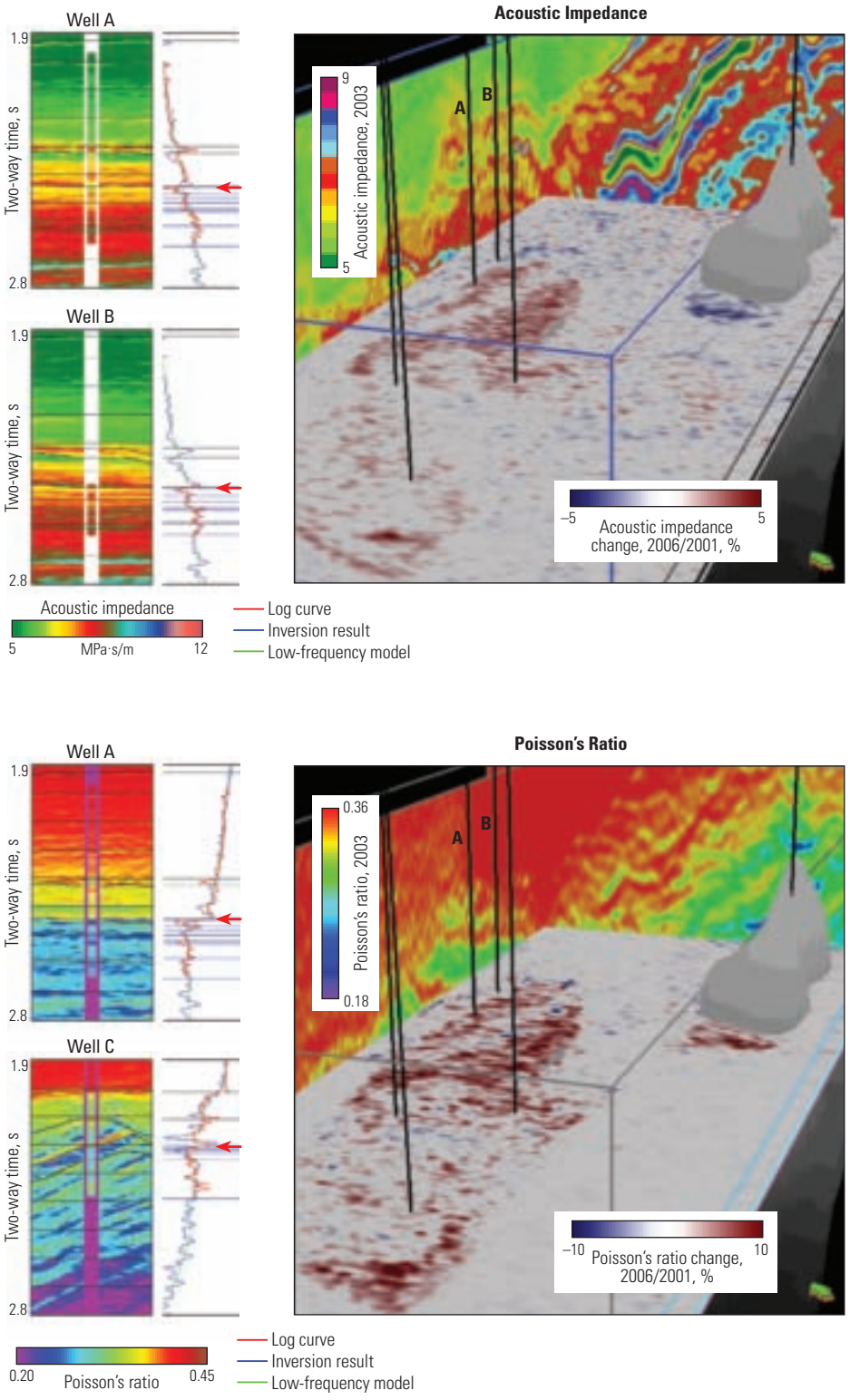

^ Time-lapse inversion. Results for acoustic impedance (*top*) and Poisson's ratio (*bottom*) use a low-frequency model based on simulation results. In the 3D volume (*top right*), the back and side panels show acoustic impedance values from the 2003 survey. The horizontal surface is a time-slice of the ratio of acoustic impedance in 2006 to that in 2001. The increase (red) has been interpreted as replacement of oil by water. Absolute acoustic impedance comparisons at two wells (*top left*) show good correlation between well measurements and the 2003 acoustic impedance values. The red arrows in each log track point to the top of the horizon of interest. The log tracks display well data (red), seismically derived values (blue) and the low-frequency model (green). Results for Poisson's ratio (*bottom*) are plotted similarly. Well C is outside the 3D volume.

15. Osdal B, Husby O, Aronsen HA, Chen N and Alsos T: "Mapping the Fluid Front and Pressure Buildup Using 4D Data on Norne Field," *The Leading Edge* 25, no. 9 (September 2006): 1134–1141.
16. Khazanehdari J, Curtis A and Goto R: "Quantitative Time-Lapse Seismic Analysis Through Prestack Inversion and Rock Physics," *Expanded Abstracts*, 75th SEG Annual International Meeting and Exposition, Houston, November 6–11, 2005: 2476–2479.
17. Aronsen HA, Osdal B, Dahl T, Eiken O, Goto R, Khazanehdari J, Pickering S and Smith P: "Time Will Tell: New Insights from Time-Lapse Seismic Data," *Oilfield Review* 16, no. 2 (Summer 2004): 6–15.
18. Murineddu A, Bertrand-Biran V, Hope T, Westeng K and Osdal B: "Reservoir Monitoring Using Time-Lapse Seismic over the Norne Field: An Ongoing Story," presented at the Norsk Petroleumsforening Biennial Geophysical Seminar, Kristiansand, Norway, March 10–12, 2008.

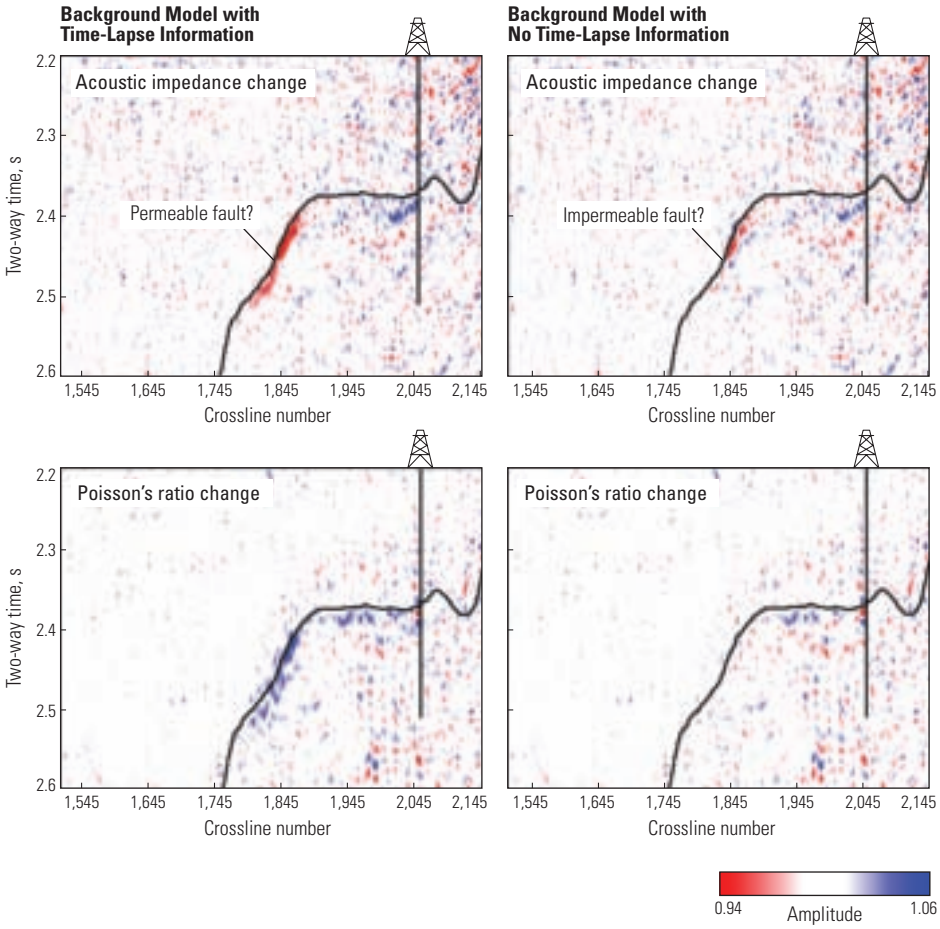

^ Effect of background models on inversion. Time-lapse inversion for acoustic impedance (*top*) and Poisson's ratio (*bottom*) shows different results using different background models. These panels focus on a region where the reservoir simulation model contains a transmissible fault that allows gas migration. The acoustic impedance section calculated with a background model that incorporated time-lapse effects (*top left*) indicates a decrease in acoustic impedance (red) across the fault. In the acoustic impedance section calculated without a time-lapse background model (*top right*), the decrease in acoustic impedance is constrained to the area above the fault, suggesting the fault is not transmissible. The inversion for Poisson's ratio also suggests a transmissible fault, but only when a background model is used that honors simulator data (*bottom left*). The black curve on each panel is the top of the formation indicated by red arrows in the previous figure. The amplitudes are the ratio of the 2004 values to the 2001 values.

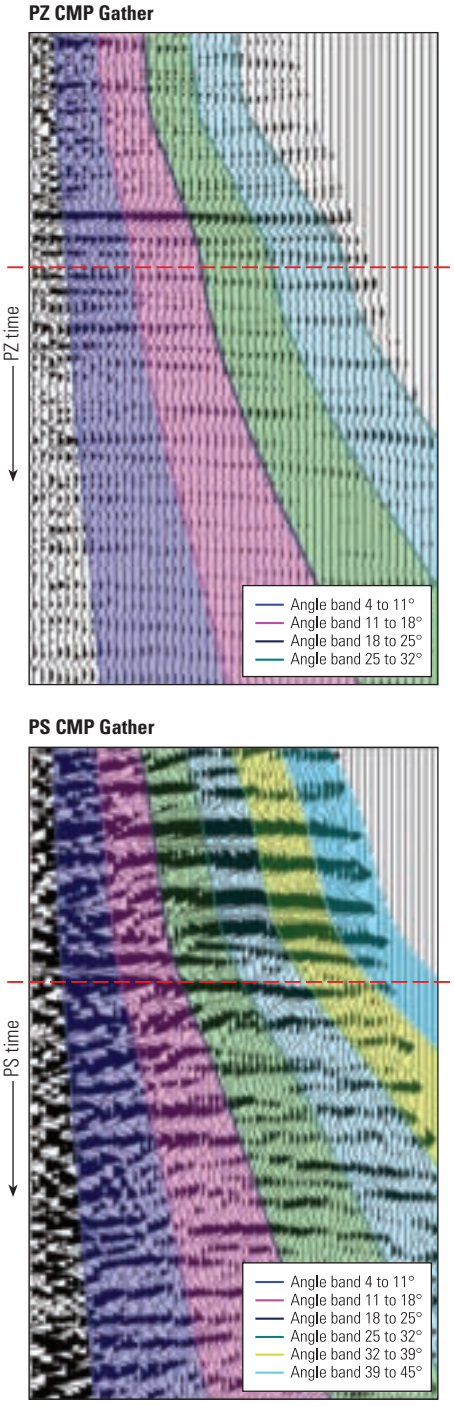

^ Multicomponent seismic data. Common midpoint (CMP) gathers of PZ (*top*) and PS (*bottom*) reflection data show traces at increasing offset from left to right. Color bands delineate angle ranges. Several reflections exhibit AVO effects, which may differ in their expressions on PZ and PS gathers. For example, in the PZ gather, the reflection at the dotted red line is slightly positive at zero offset, and decreases to nearly zero amplitude with increasing offset. Arrivals from the same reflector in the PS gather are strongly positive at zero offset and decrease gradually with increasing offset.

For the time-lapse low-frequency models, estimates of elastic properties were obtained from the ECLIPSE reservoir simulator in three steps: reservoir properties were converted from depth to time using the velocity model, then converted to elastic-property changes using rock-physics models. Finally, the spatial and temporal distributions of the property changes were constrained by seismic-velocity changes observed in time-lapse traveltime differences.

This unique combination of time-converted reservoir properties with seismic-derived traveltime changes delivered accurate changes in elastic properties consistent with the reservoir simulation. Significant differences were found between inversion results that did and did not use updated background models (above).

The StatoilHydro reservoir management team plans to use these results to track the movement of the waterflood front, evaluate the progress of water and gas injection, estimate the pressure distribution and update the reservoir model.

Multicomponent Inversion

The previous examples dealt with inversion of *P*-wave data. Towed-streamer seismic surveys are designed to generate and record only *P*-waves; *S*-waves do not propagate in fluids. Compressional waves generated by the source may convert to shear waves at the seafloor or below and then travel as such through the solid formations of the subsurface, but they must convert again to *P*-waves to travel through the water and be recorded by the receivers. Information about *S*-wave velocity and shear modulus, μ, may be

gleaned through AVO analysis, but *S*-waves themselves are not recorded.

However, it is possible to acquire *S*-wave data if the receivers are coupled to the seafloor. Ocean-bottom cables (OBCs) are designed for this purpose. Typically, these cables contain four multicomponent sensors—three geophones and a hydrophone—spaced at intervals determined by the survey requirements.[19] The geophones detect the multiple components of *S*-wave motion, and the hydrophone—like towed-streamer hydrophones—detects *P*-wave signals, designated as PP arrivals. The *P*-wave is also detected by the geophones, mainly on the vertical component, giving rise to PZ signals.

The sources used in these surveys are the same as those in towed-streamer surveys, generating *P*-waves that convert to *S*-waves at the seafloor or deeper. The resulting signals are called PS data. Although multicomponent surveys are more complex to acquire and process than single-component surveys, they provide data that single-component surveys cannot.

Schlumberger has inverted multicomponent seismic data from a gas and condensate field in the North Sea. The main objective of the inversion study was to generate elastic properties—*P*-wave impedance, V_p/V_s and density—from the seismic datasets as input for calculating large-scale geomechanical properties. The geomechanical properties would be used for building a 3D mechanical earth model (MEM).[20]

Processing of PZ and PS data is far more complex than conventional single-component dataset processing. The two data types came from the same survey, but showed many differences. For example, amplitudes, velocities and AVO behavior were markedly different between the two datasets (previous page, right).

To assess the value of the PS data, simultaneous inversion of the PZ data was compared with simultaneous inversion of the combined PZ and PS datasets (right).[21] The acoustic impedance and density derived from the PZ and PS reflection amplitudes were much better resolved and matched the well values better than those calculated from PZ arrivals alone.

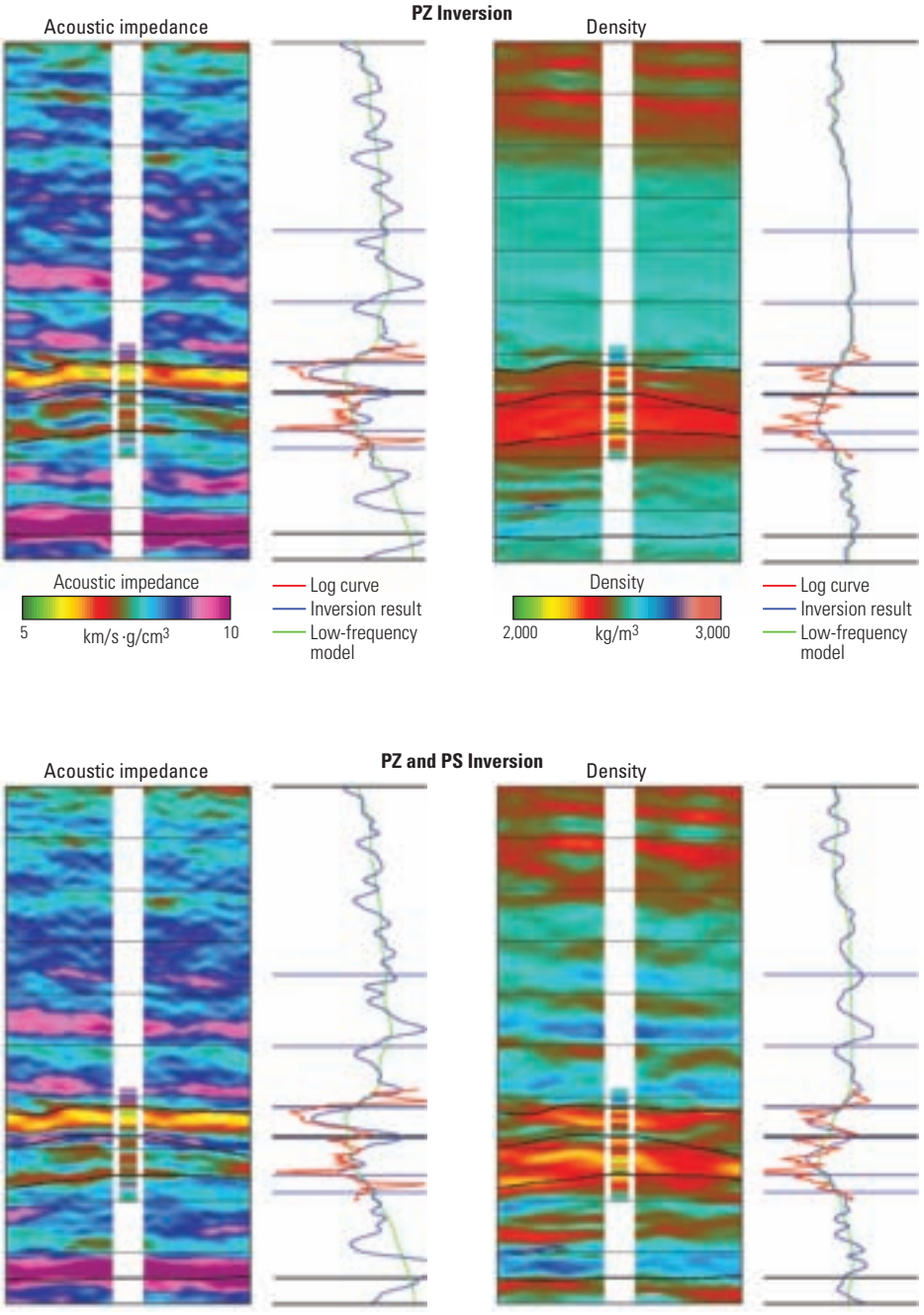

^ Simultaneous inversion of multicomponent data. Acoustic impedance (*left*) and density (*right*) from inversion using only PZ data (*top*) lack the resolution and continuity of the results of inversion using PZ and PS data (*bottom*). In particular, compared with PZ inversion, the densities predicted by inversion of PZ and PS data showed much better correlation with log values. In the panels showing inversion results, the nearly horizontal black lines are interpreted horizons. (Adapted from Rasmussen et al, reference 21.)

19. Surveys that acquire such multicomponent data are also called 4C surveys. For more on 4C surveys: Barkved O, Bartman B, Compani B, Gaiser J, Van Dok R, Johns T, Kristiansen P, Probert T and Thompson M: "The Many Facets of Multicomponent Seismic Data," *Oilfield Review* 16, no. 2 (Summer 2004): 42–56.
20. Mohamed FR, Rasmussen A, Wendt AS, Murineddu A and Nickel M: "High Resolution 3D Mechanical Earth Model Using Seismic Neural Netmodeling: Integrating Geological, Petrophysical and Geophysical Data," paper A043, prepared for presentation at the 70th EAGE Conference and Exhibition, Rome, June 9–12, 2008.
21. Rasmussen A, Mohamed FR, Murineddu A and Wendt AS: "Event Matching and Simultaneous Inversion—A Critical Input to 3D Mechanical Earth Modeling," paper P348, prepared for presentation at the 70th EAGE Conference and Exhibition, Rome, June 9–12, 2008.

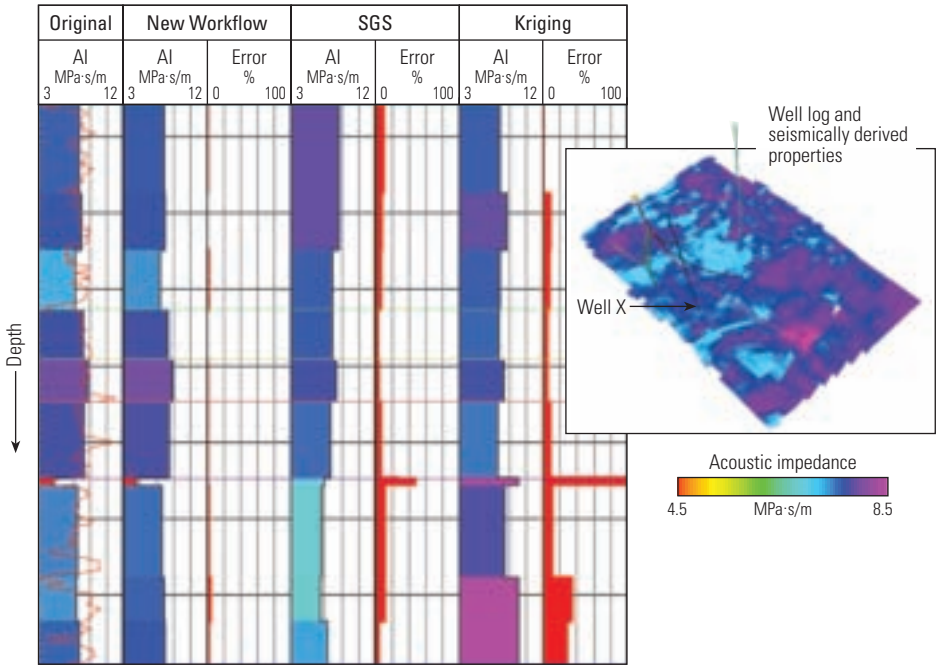

^ Acoustic properties in a 3D mechanical earth model (MEM). Seismically derived acoustic impedances helped populate a 3D MEM with mechanical properties. The inset (*right*) shows one of 10 layers in the model. Acoustic impedance (AI) values extracted along a wellbore (Well X) that had not been used in building the model (Track 1) are compared with values predicted by three methods: seismic inversion (Track 2), sequential Gaussian simulation (SGS) (Track 3) and kriging (Track 4). SGS and kriging do not use seismic data as input. Error bars (red) in each track display percentage error. The match with seismically derived acoustic impedance is significantly better than with results from the other two methods. (Adapted from Mohamed et al, reference 20.)

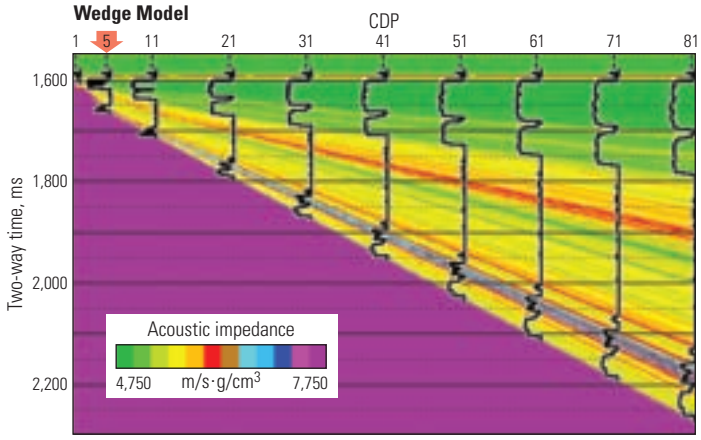

^ Wedge model of acoustic impedance. Layers thicken from left to right. Synthetic wells are shown as black curves at selected CDP numbers. The curves represent water saturations. This model was used to generate synthetic seismic sections. The acoustic impedance at CDP 5 was the basis of the background model used to invert the synthetic sections.

The acoustic impedances from seismic inversion improved the accuracy of the mechanical earth model. In a blind-well test, acoustic impedances predicted by inversion were compared with those measured in a well that had not been used for inversion calibration (left). In the 10 layers of the MEM, the well log acoustic impedances showed an extremely close match with impedances from the seismic inversion. Correlations with models built using conventional methods of generating geomechanical properties—methods that do not incorporate seismically calculated properties—did not match as well and exhibited large errors in several layers.

Looking Forward with Inversion

Seismic inversion is a powerful tool for extracting reservoir rock and fluid information from seismic data. Although most seismic surveys are designed for imaging alone, companies are increasingly applying inversion to get more out of their investments in seismic data. Some companies now perform inversion on every seismic dataset and won't drill without it.

Inversion for reservoir characterization is a multistep process that requires, in addition to the inversion algorithm itself, careful data preparation, seismic data processing, log editing and calibration, rock-property correlation and visualization. Workflows are being developed to combine these steps for optimal results.

The addition of new measurements from other disciplines, such as from deep electromagnetic sensing, promises to bring enhancements to seismic inversion results. Work on magnetotellurics and controlled-source electromagnetics for the marine environment is generating considerable interest among geophysicists, and these techniques may hold the key to detecting properties that elude seismic surveys.

Another area of potential improvement lies in enhancing the data content in seismic recordings. Low frequencies not contained in most seismic data have to be obtained or modeled from log data for inversion to absolute rock properties. However, in areas far from wells, this step may introduce unwanted bias into the results. For example, when lithologies thin, thicken, disappear or appear between wells, data from wells might not form an accurate basis for seismic models.

A new seismic data-acquisition technique is being evaluated as a means of supplying necessary low-frequency information in the absence of log data. Known as over/under

22. Camara Alfaro J, Corcoran C, Davies K, Gonzalez Pineda F, Hampson G, Hill D, Howard M, Kapoor J, Moldoveanu N and Kragh E: "Reducing Exploration Risk," *Oilfield Review* 19, no. 1 (Spring 2007): 26–43.
Moldoveanu N, Combee L, Egan M, Hampson G, Sydora L and Abriel W: "Over/Under Towed-Streamer Acquisition: A Method to Extend Seismic Bandwidth to Both Higher and Lower Frequencies," *The Leading Edge* 26, no. 1 (January 2007): 41–58.
23. Özdemir H: "Unbiased Seismic Inversion: Less Model, More Seismic," presented at the Petroleum Exploration Society of Great Britain, Geophysical Seminar, London, January 30–31, 2008.
24. Özdemir H, Leathard M and Sansom J: "Lost Frequencies Found—Almost: Inversion of Over/Under Data," paper D028, presented at the 69th EAGE Conference and Exhibition, London, June 11–14, 2007.

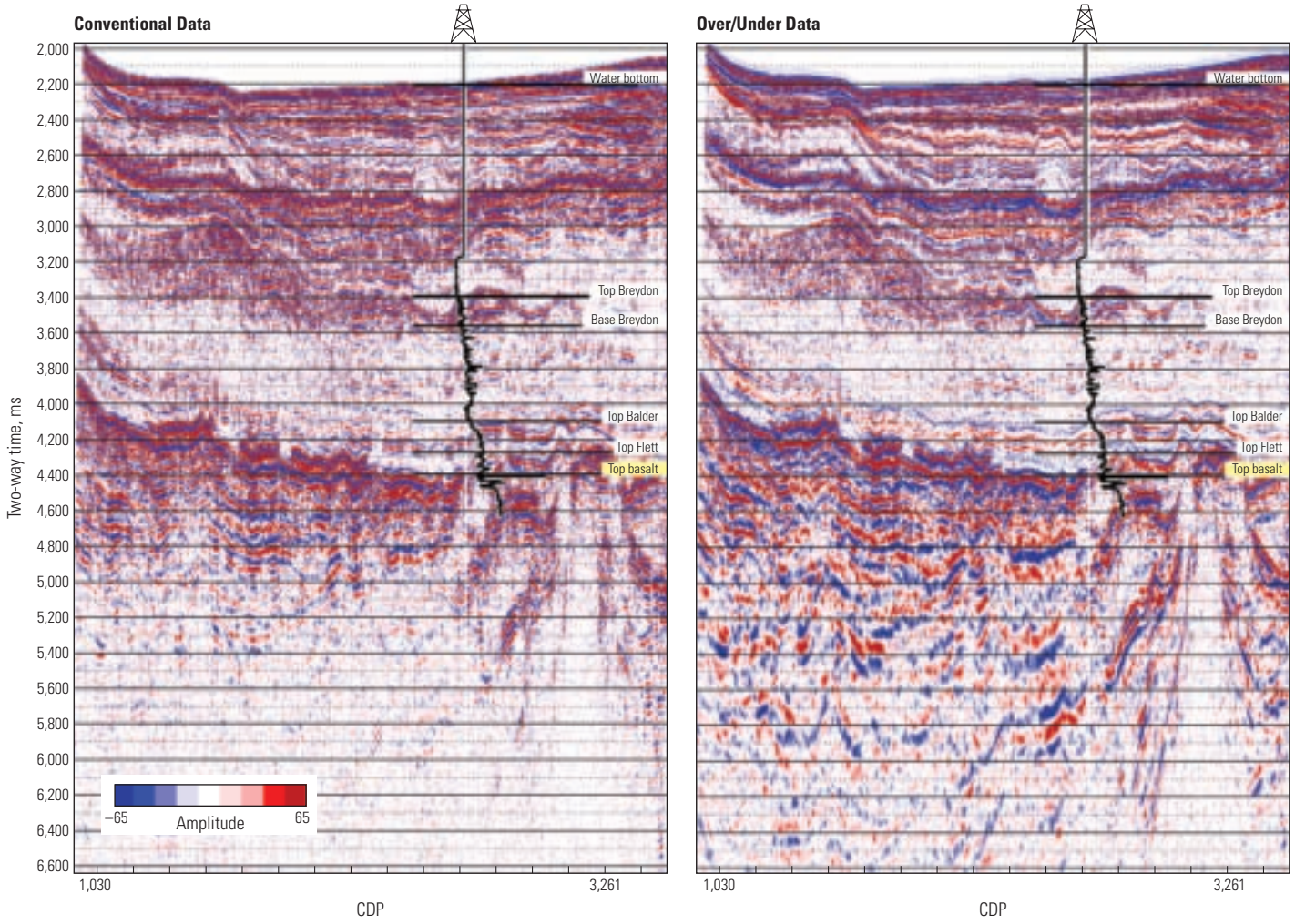

^ Seismic sections from a conventional survey with deep source and receivers (*left*) and an over/under survey (*right*). The over/under survey shows significant signal strength from deep reflectors below the basalt. In the conventional survey, the basalt blocks the penetration of seismic energy.

acquisition, the technology effectively eliminates the gaps in seismic bandwidth that plague most surveys.[22] The additional low frequencies contained in over/under data have been shown to improve imaging of deep reflectors (above). The low frequencies, often below 6 Hz, are also useful for enhancing inversion.[23]

Modeling has been used to study the impact of these additional low frequencies on seismic inversion.[24] The starting point is a wedge-shaped acoustic impedance model with reservoir intervals of varying thickness (previous page, bottom left). Two synthetic seismic sections are constructed: one with a wavelet extracted from a conventional survey and the other with a wavelet extracted from an over/under survey (right). In essence, the first

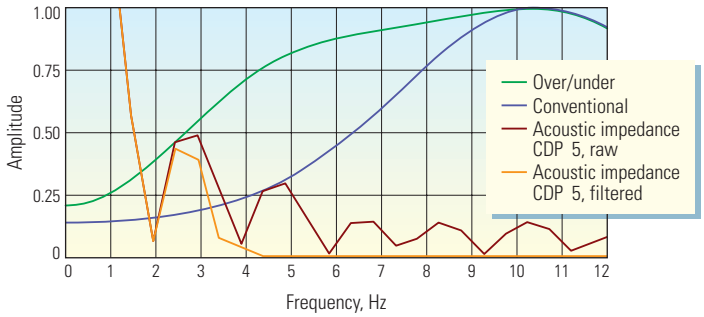

^ Spectra of conventional and over/under wavelets. The over/under wavelet (green) is richer in low frequencies, especially from 3 to 6 Hz, than the conventional wavelet (dark blue). The frequency content of the synthetic acoustic impedance log at CDP 5 of the wedge model is shown in brown. A low-pass filtered version of this log (gold) formed the background model for inversion of the synthetic seismic sections.

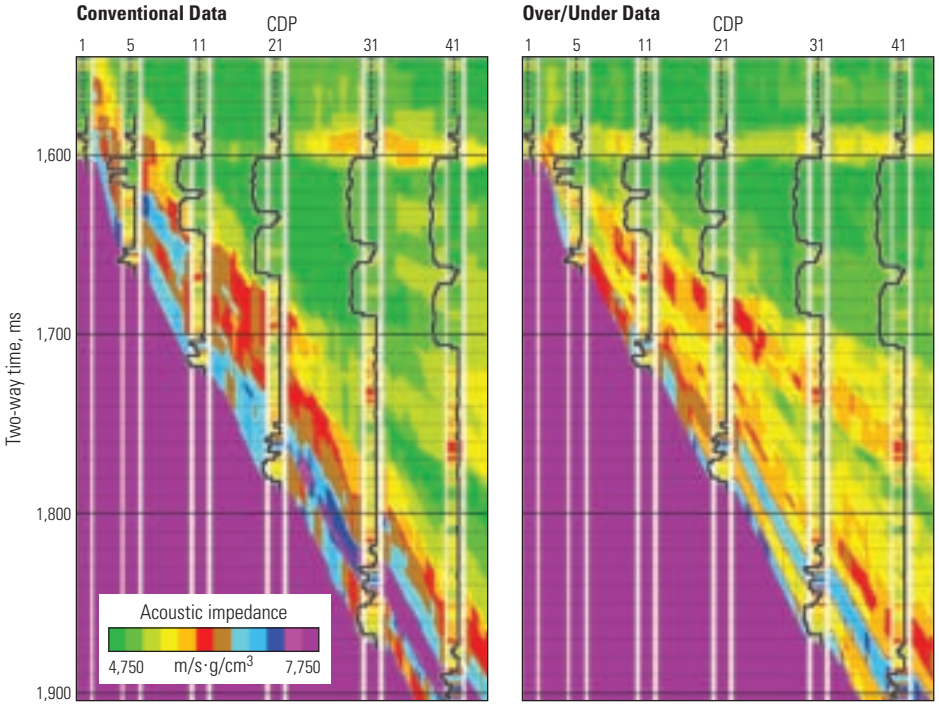

^ Inversion of synthetic conventional and over/under data. Both datasets were inverted using a background model comprising a filtered version of the acoustic impedance log at CDP 5. The over/under acoustic impedance section (*right*) delivers a wedge-shaped result that more closely matches the well information than does the conventional acoustic impedance section (*left*). The over/under version maps the low acoustic impedances (green) of the reservoir, which thickens to the right, and also produces a better match with the high acoustic impedance zones (yellow and red) below the reservoir, which also thicken to the right.

synthetic section has the frequency content of a conventional survey, and the second synthetic section has the enhanced frequency content of an over/under survey.

These synthetic seismic sections were inverted using a single low-frequency background model. The background model was created by low-pass filtering (between 0 and 3 to 4 Hz) the acoustic impedance from one well. This simulates an exploration setting in which data from only one well are available for constraining the inversion model.

Comparing inversion results of the conventional and the over/under sections shows that the acoustic impedances from the over/under section correlated much better with acoustic impedances "measured" at wells, and therefore matched the actual model better than did the results using the conventional data as input (above). The addition of data in the range from 3 to 6 Hz, supplied by the over/under technique, made a significant difference in the inversion, returning reliable rock-property information although log data were sparse.

Seismic data with a large bandwidth and high positioning accuracy also allow detection and measurement of minute stress effects in 3D and 4D seismic data.[25] For example, the effects of subsidence-induced stress have been seen in the properties of *S*-wave velocities measured by a multicomponent survey in the North Sea (next page). Seismic inversion can potentially be used to infer spatial and temporal stress changes in the subsurface from seismic data.[26] Schlumberger geophysicists envision the use of seismic inversion for determining the triaxial

25. Olofsson B, Probert T, Kommedal JH and Barkved OI: "Azimuthal Anisotropy from the Valhall 4C 3D Survey," *The Leading Edge* 22, no.12 (December 2003): 1228–1235.
Hatchell P and Bourne S: "Rocks Under Strain: Strain-Induced Time-Lapse Time Shifts Are Observed for Depleting Reservoirs," *The Leading Edge* 24, no. 12 (December 2005): 1222–1225.
Herwanger J and Horne S: "Predicting Time-Lapse Stress Effects in Seismic Data," *The Leading Edge* 24, no. 12 (December 2005): 1234–1242.
Herwanger J, Palmer E and Schiøtt CR: "Anisotropic Velocity Changes in Seismic Time-Lapse Data," presented at the 75th SEG Annual International Meeting and Exposition, San Antonio, Texas, September 23–28, 2007.
26. Sarkar D, Bakulin A and Kranz RL: "Anisotropic Inversion of Seismic Data for Stressed Media: Theory and a Physical Modeling Study on Berea Sandstone," *Geophysics* 68, no. 2 (March–April 2003): 690–704.
Sayers CM: "Monitoring Production-Induced Stress Changes Using Seismic Waves," presented at the 74th SEG Annual International Meeting and Exposition, Denver, October 10–15, 2004.

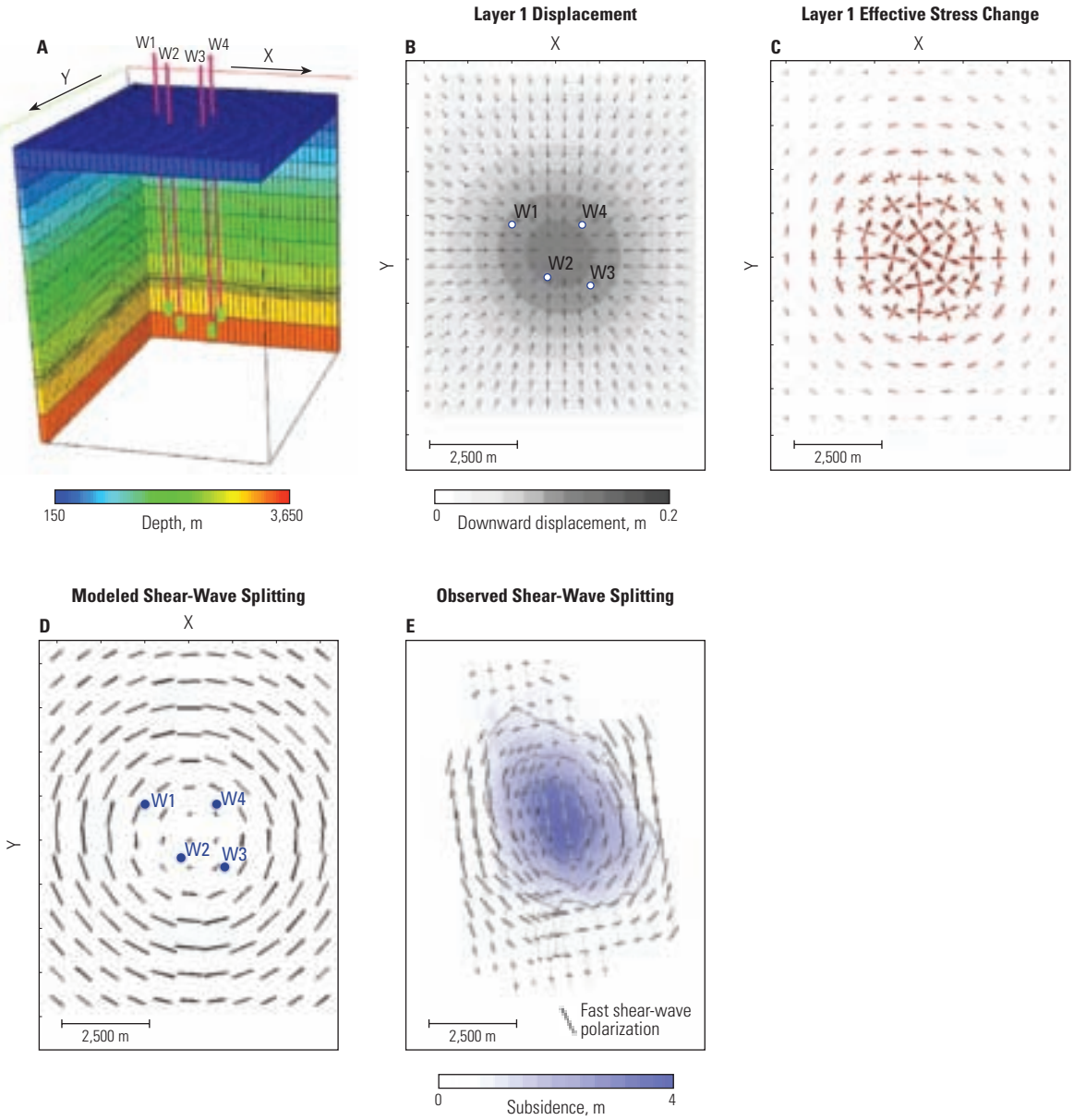

^Modeled and observed subsidence-induced shear-wave splitting in the shallow subsurface. A 3D geomechanical model (A) was constructed to investigate the effects of subsidence of a shallow layer (Layer 1, dark blue) caused by compaction of a deeper reservoir (green intervals in Wells W1, W2, W3 and W4) under production. The resulting ground displacement in the shallow subsurface causes a nearly circular subsidence bowl (B). Changes in effective stress associated with the modeled deformation (C) are greatest in the center of the bowl. These stress changes give rise to elastic anisotropy, which in turn causes shear-wave splitting, a phenomenon in which two orthogonally polarized shear waves propagate at different speeds. The largest shear-wave splitting occurs at the flanks of the subsidence bowl (D), where the difference between the horizontal stresses is largest. At the center of the subsidence bowl, where horizontal stress changes are large but isotropic, shear-wave splitting is minimal. The azimuth of the bars shows the polarization direction of the fast shear wave, and the length of each bar is proportional to the time lag between fast and slow shear waves. Observed shear-wave splitting in a subsidence bowl over a compacting North Sea reservoir (E) follows a pattern similar to the modeled phenomenon.

stress state of the reservoir and overburden as a function of time. This knowledge can be used to plan well trajectories and anticipate wellbore failure and rock damage. Characterizing mechanical properties of the overburden and monitoring stress changes over time open a new field of application for seismic inversion.

Seismically derived rock and fluid properties are playing an increasing role in characterization of geological models, and therefore extend naturally into the domain of the reservoir production simulator. This characterization of rock properties can be extended into the overburden. The next steps in the progression of seismic inversion will include increasing use of reservoir and geomechanical simulation results to generate starting models for inversion, and vice versa. Closing this loop and operating in real time on time-lapse data will take seismic inversion far beyond reading between the lines to reading between wells. —LS